# Towards a Better Understanding of Large Scale Network Models

Guoqiang Mao, *Senior Member, IEEE,* and Brian D.O. Anderson, *Life Fellow, IEEE*



**Abstract**

Connectivity and capacity are two fundamental properties of wireless multi-hop networks. The scalability of these properties has been a primary concern for which asymptotic analysis is a useful tool. Three related but logically distinct network models are often considered in asymptotic analyses, viz. the dense network model, the extended network model and the infinite network model, which consider respectively a network deployed in a fixed finite area with a sufficiently large node density, a network deployed in a sufficiently large area with a fixed node density, and a network deployed in $\Re^2$ with a sufficiently large node density. The infinite network model originated from continuum percolation theory and asymptotic results obtained from the infinite network model have often been applied to the dense and extended networks. In this paper, through two case studies related to network connectivity on the expected number of isolated nodes and on the vanishing of components of finite order $k > 1$ respectively, we demonstrate some subtle but important differences between the infinite network model and the dense and extended network models. Therefore extra scrutiny has to be used in order for the results obtained from the infinite network model to be applicable to the dense and extended network models. Asymptotic results are also obtained on the expected number of isolated nodes, the vanishingly small impact of the boundary effect on the number of isolated nodes and the vanishing of components of finite order $k > 1$ in the dense and extended network models using a generic random connection model.

**Index Terms**

Dense network model, extended network model, infinite network model, continuum percolation, connectivity, random connection model

## I. Introduction

Wireless multi-hop networks in various forms, e.g. wireless ad hoc networks, sensor networks, mesh networks and vehicular networks, have been the subject of intense research in the recent decades (see [1] and references therein). Connectivity and capacity are two fundamental properties of these networks. The scalability of these properties as the number of nodes in the network becomes sufficiently large has been a primary concern. Asymptotic analysis, valid when the number of nodes in the network is large enough, has been useful for understanding the characteristics of these networks.

Three related but logically distinct network models have been widely used in the asymptotic analysis of large scale multi-hop networks. The first model, often referred to as the *dense network model*, considers that the network is deployed in a finite area with a sufficiently large node density. The second model, often referred to as the *extended network model*, considers that the node density is fixed and the network area is sufficiently large. The third model, referred to as the *infinite network model*, has its origin in continuum percolation theory [2]. It considers a network deployed in an infinite area, i.e. $\Re^2$ in 2D, and analyzes the properties of the network as the node density becomes sufficiently large. Due to the relatively longer history of research into continuum percolation theory and relatively abundant results in that area, and the close connections between the infinite network model and the dense and extended network models, results obtained in the infinite network model are often applied straightforwardly to the first and second models [3]–[8].

In this paper, through two case studies on key events related to the network connectivity, i.e. the expected number of isolated nodes and the vanishing of components of fixed and finite order $k > 1$ (the order of a component refers to the number of nodes in the component), using a random connection model, we demonstrate some subtle but important differences between the infinite network model and the dense and extended network models due to the *truncation effect*, to be explained in the following paragraphs. Therefore results obtained from an infinite network model *cannot be directly applied* to the dense and extended networks. Instead some careful analysis of the impact of the truncation effect is required.

Here we give a detailed explanation of the above comments using a *unit disk connection model* as an example[1]. Under the *unit disk connection model*, two nodes are directly connected if and only if (iff) their Euclidean distance is smaller than or equal to a given threshold $r(\rho)$, a parameter which is often taken as a function of a further parameter $\rho$, to be defined shortly, under the dense and extended network models; the parameter $r(\rho)$ is termed the *transmission range*. The dense and extended

G. Mao is with the School of Electrical and Information Engineering, the University of Sydney and National ICT Australia. Email: guoqiang.mao@sydney.edu.au.

B.D.O. Anderson is with the Research School of Information Sciences and Engineering, Australian National University and National ICT Australia. Email: brian.anderson@anu.edu.au.

This research is funded by ARC Discovery project: DP0877562.

[1]In the paper, we have omitted some trivial discussions on the difference between Poisson and uniform distributions and consider Poisson node distribution only.

network models that are often considered assume respectively a) nodes are Poissonly distributed in a unit area, say a square, with density $\rho$ and $r(\rho) = \sqrt{\frac{\log \rho + c}{\pi \rho}}$ (the dense network model); b) nodes are Poissonly distributed on a square $\sqrt{\rho} \times \sqrt{\rho}$ with density 1 and $r(\rho) = \sqrt{\frac{\log \rho + c}{\pi}}$ (the extended network model). The parameter $c$ may be either a constant; or it can depend on $\rho$, in which case $c = o(\log \rho)$. The corresponding infinite network model considers nodes Poissonly distributed in $\Re^2$ with density $\rho$ and a pair of nodes are directly connected iff their Euclidean distance is smaller than or equal to $r$, which *does not* depend on $\rho$. The dense network model can be converted into the extended network model by scaling the Euclidean distances between *all pairs* of nodes by a factor of $\sqrt{\rho}$ while maintaining their connections, and conversely. Therefore the dense network model and the extended network model are equivalent in the analysis of connectivity. In the extended network model, as $\rho \to \infty$, the network area approaches $\Re^2$ and the average node degree approaches infinity following $\Theta(\log \rho)$, i.e. a node has more and more connections as $\rho \to \infty$. This resembles the situation that occurs in the infinite network model as $\rho \to \infty$. This close connection between the infinite network model and the dense and extended network models creates the *illusion* that as $\rho \to \infty$ results obtained in the infinite network model can also be applied directly to the dense and extended models, e.g. those dealing with the vanishing of isolated nodes, the uniqueness of the component of infinite order, the vanishing of components of finite order $k > 1$ [3]–[8].

Starting from the dense network model however, if we scale the Euclidean distances between all pairs of nodes by a factor $1/\sqrt{\frac{\log \rho + c}{\pi \rho}}$, there results a network on a square $1/\sqrt{\frac{\log \rho + c}{\pi \rho}} \times 1/\sqrt{\frac{\log \rho + c}{\pi \rho}}$ with node density $\frac{\log \rho + c}{\pi}$, where $\frac{\log \rho + c}{\pi} \to \infty$ as $\rho \to \infty$, and a pair of nodes are directly connected iff their Euclidean distance is equal to or smaller than $r = 1$, *independently* of the node density. This latter network model is also equivalent to the dense and extended network models in connectivity. On the other hand, this latter network can also be obtained from an infinite network on $\Re^2$ with node density $\frac{\log \rho + c}{\pi}$ and $r = 1$ by removing all nodes and the associated connections outside a square of $1/\sqrt{\frac{\log \rho + c}{\pi \rho}} \times 1/\sqrt{\frac{\log \rho + c}{\pi \rho}}$ in $\Re^2$. We term the effect associated with the above removal procedure as the *truncation effect*. From the above discussion, it is clear that a prerequisite for the results obtained in the infinite network model to be applicable to the dense or extended network models is that the impact of the truncation effect on the property concerned must be vanishingly small as $\rho \to \infty$.

The main contributions of this paper are:

- Through two case studies, one on the expected number of isolated nodes and the other on the vanishing of components of fixed and finite order $k > 1$, using a random connection model, we show however that ensuring the impact of the truncation effect is vanishingly small either requires imposing a stronger requirement on the connection function or needs some non-trivial analysis to rule out the possibility of occurrence of some events associated with the truncation effect. Therefore results obtained assuming an infinite network model *cannot* be applied directly to the dense and extended network models.
- In particular, we show that in order for the impact of the truncation effect on the number of isolated nodes to be vanishingly small, a stronger requirement on the connection function (than the usual requirements of rotational invariance, integral boundedness and non-increasing monotonicity) needs to be imposed.
- We show that some non-trivial analysis is required to rule out the possibility of occurrence of some events associated with the truncation effect in order to establish the result on the vanishing of components of components of fixed and finite order $k > 1$ in the dense and extended network models. For example, an infinite component in $\Re^2$ may, after truncation, yield multiple *components of extremely large order*[2], finite components of fixed order $k > 1$ and isolated nodes in $1/\sqrt{\frac{\log \rho + c}{\pi \rho}} \times 1/\sqrt{\frac{\log \rho + c}{\pi \rho}}$, where these components are only connected via nodes and associated connections in the infinite component but outside $1/\sqrt{\frac{\log \rho + c}{\pi \rho}} \times 1/\sqrt{\frac{\log \rho + c}{\pi \rho}}$. Thus the dense and extended networks may still possibly have finite components of order $k > 1$ even though the infinite network can be shown to *asymptotically almost surely* have no such finite components as $\rho \to \infty$.
- Asymptotic results are established on the expected number of isolated nodes, the vanishingly small impact of the boundary effect on the number of isolated nodes and the vanishing of components of finite order $k > 1$ in the dense and extended network models using a generic random connection model. These results form key steps in extending asymptotic results on network connectivity from the unit disk model to the more generic random connection model.

To our knowledge, this is the first paper that has provided solid theoretical analysis to explain the difference between the infinite network model and the dense and extended network models and the cause of this difference, i.e. it is attributable to the truncation effect, which is different from the boundary effect that has been widely studied.

The rest of the paper is organized as follows. Section II reviews related work. Section III gives a formal definition of the network models, symbols and notations considered in the paper. Section IV comparatively studies the expected number of isolated nodes in a dense (or extended) network and in its counterpart infinite network model. Through the study, it shows that under certain conditions the impact of the truncation effect on the expected number of isolated nodes is non-negligible

[2]It is trivial to show that for any finite $\rho$, *almost surely* there is no infinite component in a network whose nodes are Poissonly distributed with density $\frac{\log \rho + c}{\pi}$ on a square of $1/\sqrt{\frac{\log \rho + c}{\pi \rho}} \times 1/\sqrt{\frac{\log \rho + c}{\pi \rho}}$. Therefore we use the term *components of extremely large order* to refer to those components whose order may become *asymptotically infinite* as $\rho \to \infty$.

or may even be the dominant factor. Section V first gives an example to show that asymptotic vanishing of components of fixed and finite order $k > 1$ in an infinite network does not carry straightforwardly the conclusion that components of fixed and finite order $k > 1$ also vanish asymptotically in the dense and extended networks. Then to fill this theoretical gap and with a supplementary condition holding, a result is presented on the asymptotic vanishing of components of fixed and finite order $k > 1$ in the dense and extended network models under a random connection model. Finally Section VI summarizes conclusions and future work.

## II. Related Work

Extensive research has been done on connectivity problems using the well-known random geometric graph and the unit disk connection model, which is usually obtained by randomly and uniformly distributing $n$ vertices in a given area and connecting any two vertices iff their distance is smaller than or equal to a given threshold $r(n)$ [9], [10]. Significant outcomes have been obtained [3], [10]–[16].

Penrose [17], [18] and Gupta et al. [3] proved using different techniques that if the transmission range is set to $r(n) = \sqrt{\frac{\log n + c(n)}{\pi n}}$, a random network formed by uniformly placing $n$ nodes in a unit-area disk in $\Re^2$ is asymptotically almost surely connected as $n \to \infty$ iff $c(n) \to \infty$. Specifically, Penrose's result is based on the fact that in the above random network as $\rho \to \infty$ the longest edge of the minimum spanning tree converges in probability to the minimum transmission range required for the above random network to have no isolated nodes (or equivalently the longest edge of the nearest neighbor graph of the above network) [10], [17], [18]. Gupta and Kumar's result is based on a key finding in continuum percolation theory [2, Chapter 6]: Consider an *infinite network* with nodes distributed on $\Re^2$ following a Poisson distribution with density $\rho$; and suppose that a pair of nodes separated by a Euclidean distance $x$ are directly connected with probability $g(x)$, independent of the event that another distinct pair of nodes are directly connected. Here, $g : \Re^+ \to [0, 1]$ satisfies the conditions of rotational invariance, non-increasing monotonicity and integral boundedness [2, pp. 151-152]. As $\rho \to \infty$ *asymptotically almost surely* the above network on $\Re^2$ has only a unique infinite component and isolated nodes.

In [12], Philips et al. proved that the average node degree, i.e. the expected number of neighbors of an arbitrary node, must grow logarithmically with the area of the network to ensure that the network is connected, where nodes are placed randomly on a square according to a Poisson point process with a known density in $\Re^2$. This result by Philips et al. actually provides a necessary condition on the average node degree required for connectivity. In [11], Xue et al. showed that in a network with a total of $n$ nodes randomly and uniformly distributed in a unit square in $\Re^2$, if each node is connected to $c \log n$ nearest neighbors with $c \leq 0.074$ then the resulting random network is asymptotically almost surely disconnected as $n \to \infty$; and if each node is connected to $c \log n$ nearest neighbors with $c \geq 5.1774$ then the network is asymptotically almost surely connected as $n \to \infty$. In [14], Balister et al. advanced the results in [11] and improved the lower and upper bounds to $0.3043 \log n$ and $0.5139 \log n$ respectively. In a more recent paper [16], Balister et al. achieved much improved results by showing that there exists a constant $c_{crit}$ such that if each node is connected to $\lfloor c \log n \rfloor$ nearest neighbors with $c < c_{crit}$ then the network is asymptotically almost surely disconnected as $n \to \infty$, and if each node is connected to $\lfloor c \log n \rfloor$ nearest neighbors with $c > c_{crit}$ then the network is asymptotically almost surely connected as $n \to \infty$. In both [14] and [16], the authors considered nodes randomly distributed following a Poisson process of intensity one in a square of area $n$ in $\Re^2$. In [13], Ravelomanana investigated the critical transmission range for connectivity in 3-dimensional wireless sensor networks and derived similar results to the 2-dimensional results in [3].

All the above work is based on the unit disk connection model. The unit disk connection model may simplify analysis but no real antenna has an antenna pattern similar to it. The log-normal shadowing connection model, which is more realistic than the unit disk connection model, has accordingly been considered for investigating network connectivity in [19]–[24]. Under the log-normal shadowing connection model, two nodes are directly connected if the received power at one node from the other node, whose attenuation follows the log-normal model [25], is greater than a given threshold. In [19]–[24], the authors investigated from different perspectives the necessary condition for a network with nodes uniformly or Poissonly distributed in a bounded area in $\Re^2$ and a pair of nodes are directly connected following the log-normal connection model to be connected. Most of the above work is based on the observation that a necessary condition for a connected network is that the network has no isolated nodes. Their analysis [19]–[24] also relies on the assumption that under the log-normal connection model, the node isolation events are independent, an assumption yet to be validated analytically.

Other work in the area include [5], [6], [8], [26], which studies from the percolation perspective, the impact of mutual interference caused by simultaneous transmissions, the impact of physical layer cooperative transmissions, the impact of directional antennas and the impact of unreliable links on connectivity respectively.

In this paper we discuss the relation between three widely used network models in the above studies, i.e. the dense network model, the extended network model and the infinite network model which originated from continuum percolation theory. We examine mainly from the connectivity perspective the similarities and differences between these models and demonstrate that results obtained from continuum percolation theory assuming an infinite network model *cannot* be directly applied to the dense and extended network models. We also establish some results that form key steps in extending asymptotic results on network connectivity from the unit disk model to the more generic random connection model.

## III. Network Models

In this section we give a formal definition of network models considered in the paper. Let $g : \Re^{+} \to [0,1]$ be a function satisfying the conditions of non-increasing monotonicity and integral boundedness [3], [4]:

$$g(x) \leq g(y) \qquad \text{whenever } \ x \geq y \tag{1}$$

$$0 < \int_{\Re^2} g(\|\boldsymbol{x}\|)\, d\boldsymbol{x} < \infty \tag{2}$$

where $\|\boldsymbol{x}\|$ denotes the Euclidean norm of $\boldsymbol{x}$. The function $g$ is the connection function that has been widely considered in the random connection model [2], [27, Chapter 6]. Further the requirement of rotational invariance on the connection function in the random connection model [2], [27, Chapter 6] has been met implicitly by letting $g$ be a function of a scalar, typically representing the Euclidean distance between two nodes being considered.

The following notations and definitions are used throughout the paper:

- $f(z) = o_z(h(z))$ iff $\lim_{z\to\infty} \frac{f(z)}{h(z)} = 0$;
- $f(z) = \omega_z(h(z))$ iff $h(z) = o_z(f(z))$;
- $f(z) = \Theta_z(h(z))$ iff there exist a sufficiently large $z_0$ and two positive constants $c_1$ and $c_2$ such that for any $z > z_0$, $c_1 h(z) \geq f(z) \geq c_2 h(z)$;
- $f(z) \sim_z h(z)$ iff $\lim_{z\to\infty} \frac{f(z)}{h(z)} = 1$;
- An event $\xi$ is said to occur almost surely if its probability equals to one;
- An event $\xi_z$ depending on $z$ is said to occur asymptotically almost surely (a.a.s.) if its probability tends to one as $z \to \infty$.

The above definition applies whether the argument $z$ is continuous or discrete, e.g. assuming integer values.

Using the integral boundedness condition on $g$ and the non-increasing property of $g$, it can be shown that

$$\int_{\Re^2} g(\|\boldsymbol{x}\|)\, d\boldsymbol{x} \quad = \quad \lim_{z\to\infty} \int_0^z 2\pi x g(x)\, dx$$

and

$$\lim_{z\to\infty} \int_z^\infty 2\pi x g(x)\, dx = 0$$

The above equation, together with the following derivations

$$\begin{aligned}
& \lim_{z\to\infty} \int_z^\infty 2\pi x g(x)\, dx \\
\geq \quad & \lim_{z\to\infty} \int_z^{2z} 2\pi x g(x)\, dx \\
\geq \quad & \lim_{z\to\infty} \int_z^{2z} 2\pi x g(2z)\, dx \\
= \quad & \lim_{z\to\infty} 3\pi z^2 g(2z)
\end{aligned}$$

allow us to conclude that

$$g(x) = o_x\left(\frac{1}{x^2}\right) \tag{3}$$

From time to time, we may require $g$ to satisfy the more restrictive requirement that

$$g(x) = o_x\left(\frac{1}{x^2 \log^2 x}\right) \tag{4}$$

and (1). When we do impose such additional constraint, we will specify it clearly. It is obvious that conditions (1) and (2) imply (3) while condition (4) implies (2) and (3).

In the following analysis, we will only use (1) and (4) (instead of (1) and (2)) when necessary. This helps to identify which part of the analysis relies on the more restrictive requirement on $g$. In our analysis, we assume that $g$ has infinite support when necessary. Our results however apply to the situation when $g$ has bounded support, which forms a special case and only makes the analysis easier.

Further, define

$$r_\rho \triangleq \sqrt{\frac{\log\rho + b}{C\rho}} \tag{5}$$

[3]Throughout this paper, we use the non-bold symbol, e.g. $x$, to denote a scalar and the bold symbol, e.g. $\boldsymbol{x}$, to denote a vector.

[4]We refer readers to [2], [27, Chapter 6] for detailed discussions on the random connection model.

for some non-negative value $\rho$, where

$$0 < C = \int_{\Re^2} g\left(\|\boldsymbol{x}\|\right) d\boldsymbol{x} < \infty \tag{6}$$

and $b$ is a constant ($+\infty$ is allowed).

In the following, we give the formal definitions of four network models discussed in the paper. The motivation for defining a new model in Definition 3 appears later after all models are defined.

*Definition 1:* (dense network model) Let $\mathcal{G}\left(\mathcal{X}_\rho, g_{r_\rho}, A\right)$ be a network with nodes Poissonly distributed on a unit square $A \triangleq \left[-\frac{1}{2}, \frac{1}{2}\right]^2$ with density $\rho$ and a pair of nodes separated by a Euclidean distance $x$ are directly connected with probability $g_{r_\rho}\left(x\right) \triangleq g\left(\frac{x}{r_\rho}\right)$, independent of the event that another distinct pair of nodes are directly connected. $\mathcal{X}_\rho$ denotes the vertex set in $\mathcal{G}\left(\mathcal{X}_\rho, g_{r_\rho}, A\right)$.

*Definition 2:* (extended network model) Let $\mathcal{G}\left(\mathcal{X}_1, g_{\sqrt{\frac{\log\rho+b}{C}}}, A_{\sqrt{\rho}}\right)$ be a network with nodes Poissonly distributed on a square $A_{\sqrt{\rho}} \triangleq \left[-\frac{\sqrt{\rho}}{2}, \frac{\sqrt{\rho}}{2}\right]^2$ with density 1 and a pair of nodes separated by a Euclidean distance $x$ are directly connected with probability $g_{\sqrt{\frac{\log\rho+b}{C}}}\left(x\right) \triangleq g\left(\frac{x}{\sqrt{\frac{\log\rho+b}{C}}}\right)$, independent of the event that another distinct pair of nodes are directly connected. $\mathcal{X}_1$ denotes the vertex set in $\mathcal{G}\left(\mathcal{X}_1, g_{\sqrt{\frac{\log\rho+b}{C}}}, A_{\sqrt{\rho}}\right)$.

*Definition 3:* Let $\mathcal{G}\left(\mathcal{X}_{\frac{\log\rho+b}{C}}, g, A_{\frac{1}{r_\rho}}\right)$ be a network with nodes Poissonly distributed on a square $A_{\frac{1}{r_\rho}} \triangleq \left[-\frac{1}{2r_\rho}, \frac{1}{2r_\rho}\right]^2$ with density $\frac{\log\rho+b}{C}$ and a pair of nodes separated by a Euclidean distance $x$ are directly connected with probability $g\left(x\right)$, independent of the event that another distinct pair of nodes are directly connected. $\mathcal{X}_{\frac{\log\rho+b}{C}}$ denotes the vertex set in $\mathcal{G}\left(\mathcal{X}_{\frac{\log\rho+b}{C}}, g, A_{\frac{1}{r_\rho}}\right)$.

*Definition 4:* (infinite network model) Let $\mathcal{G}\left(\mathcal{X}_\rho, g, \Re^2\right)$ be a network with nodes Poissonly distributed on $\Re^2$ **with density** $\rho$ and a pair of nodes separated by a Euclidean distance $x$ are directly connected with probability $g\left(x\right)$, independent of the event that another distinct pair of nodes are directly connected. $\mathcal{X}_\rho$ denotes the vertex set in $\mathcal{G}\left(\mathcal{X}_\rho, g, \Re^2\right)$.

With minor abuse of the terminology, we use $A$ (respectively $A_{\sqrt{\rho}}$, $A_{\frac{1}{r_\rho}}$) to denote both the square itself and the area of the square, and in the latter case, $A = 1$ (respectively $A_{\sqrt{\rho}} = \rho$, $A_{\frac{1}{r_\rho}} = \frac{1}{r_\rho^2}$).

The reason for choosing this particular form of $r_\rho$ and the above network models is to avoid triviality in the analysis and to make the analysis compatible with existing results obtained under a unit disk connection model. Particularly when $g$ takes the form that $g(x) = 1$ for $x \leq 1$ and $g(x) = 0$ for $x > 1$, it can be shown that $\mathcal{G}\left(\mathcal{X}_\rho, g_{r_\rho}, A\right)$ reduces to the dense network model under a unit disk connection model discussed in [3], [10], [27] where $C = \pi$ and $r_\rho$ corresponds to the critical transmission range for connectivity; $\mathcal{G}\left(\mathcal{X}_1, g_{\sqrt{\frac{\log\rho+b}{C}}}, A_{\sqrt{\rho}}\right)$ reduces to the extended network model under a unit disk connection model considered in [27], [28, Chapter 3.3.2]. Thus the above model easily incorporates the unit disk connection model as a special case. A similar conclusion can also be drawn for the log-normal connection model.

Now we establish the relationship between the three network models in Definitions 1, 2, 3 on finite and then asymptotically infinite regions respectively using the scaling and coupling technique [2]. Given an instance of $\mathcal{G}\left(\mathcal{X}_\rho, g_{r_\rho}, A\right)$, if we scale the Euclidean distances between *all pairs* of nodes by a factor of $\sqrt{\rho}$ while maintaining their connections, there results a random network where nodes are Poissonly distributed on a square $A_{\sqrt{\rho}}$ with density 1 and a pair of nodes separated by a Euclidean distance $x$ are directly connected with probability $g_{\sqrt{\frac{\log\rho+b}{\rho}}}(x)$, i.e. an instance of $\mathcal{G}\left(\mathcal{X}_1, g_{\sqrt{\frac{\log\rho+b}{C}}}, A_{\sqrt{\rho}}\right)$. All connectivity properties, e.g. connectivity, number of isolated nodes, number of components of a specified order, that hold in the instance of $\mathcal{G}\left(\mathcal{X}_\rho, g_{r_\rho}, A\right)$ are also valid for the associated instance in $\mathcal{G}\left(\mathcal{X}_1, g_{\sqrt{\frac{\log\rho+b}{C}}}, A_{\sqrt{\rho}}\right)$ (To be more precise, the *underlying graphs* of these two network instances are *isomorphic* [29], [30]). Similarly if we shrink the Euclidean distances between all pairs of nodes in a network, which is an instance of $\mathcal{G}\left(\mathcal{X}_1, g_{\sqrt{\frac{\log\rho+b}{C}}}, A_{\sqrt{\rho}}\right)$, by a factor of $\frac{1}{\sqrt{\rho}}$, there results an instance of $\mathcal{G}\left(\mathcal{X}_\rho, g_{r_\rho}, A\right)$ and the two networks again have the same connectivity property. Therefore $\mathcal{G}\left(\mathcal{X}_\rho, g_{r_\rho}, A\right)$ and $\mathcal{G}\left(\mathcal{X}_1, g_{\sqrt{\frac{\log\rho+b}{C}}}, A_{\sqrt{\rho}}\right)$ are *equivalent* in that any connectivity property that holds in one model will necessarily hold in the other. Similarly, it can also be shown that $\mathcal{G}\left(\mathcal{X}_\rho, g_{r_\rho}, A\right)$ and $\mathcal{G}\left(\mathcal{X}_{\frac{\log\rho+b}{C}}, g, A_{\frac{1}{r_\rho}}\right)$ are equivalent in their connectivity properties. Thus in this paper we only chose one model, i.e. $\mathcal{G}\left(\mathcal{X}_{\frac{\log\rho+b}{C}}, g, A_{\frac{1}{r_\rho}}\right)$, to discuss the connectivity properties of finite and asymptotically infinite networks. The reason for choosing this network model is that under the model, a pair of nodes are directly connected following $g$, in the same way as nodes in the infinite network model $\mathcal{G}\left(\mathcal{X}_\rho, g, \Re^2\right)$ are directly connected. This facilitates the discussion and comparison between the finite (asymptotically infinite) network model and the infinite network model, which is a key focus of the paper.

Further, we point out that the above discussion on the equivalence of network models $\mathcal{G}\left(\mathcal{X}_\rho, g_{r_\rho}, A\right)$, $\mathcal{G}\left(\mathcal{X}_1, g_{\sqrt{\frac{\log\rho+b}{C}}}, A_{\sqrt{\rho}}\right)$ and $\mathcal{G}\left(\mathcal{X}_{\frac{\log\rho+b}{C}}, g, A_{\frac{1}{r_\rho}}\right)$ is only valid for the random connection model. For the other widely used model, i.e. the SINR

model, under some special circumstances, e.g. the background noise is negligible [1] and the attenuation function is a power law function, the three network models are equivalent; otherwise under more general conditions, *the three models are not equivalent* (see e.g. [26], [31]). However the key observation revealed in our analysis, i.e. results obtained from an infinite network model do not necessarily apply to the dense and extended network models, also holds for the SINR model.

## IV. A Comparative Study of The Expected Number of Isolated Nodes

In this section we comparatively study the expected number of isolated nodes in $\mathcal{G}\left(\mathcal{X}_{\frac{\log\rho+b}{C}}, g, A_{\frac{1}{r_\rho}}\right)$ and the expected number of isolated nodes in its counterpart in an infinite network, i.e. a region with the same area as $A_{\frac{1}{r_\rho}}$ in an infinite network on $\Re^2$ with the same node density $\frac{\log\rho+b}{C}$ and connection function $g$. The number of isolated nodes is a key parameter in the analysis of network connectivity. A necessary condition for a network to be connected is that the network has no isolated node. Such a necessary condition has been shown to be also a sufficient condition for a connected network as $\rho\to\infty$ under a unit disk connection model [10] and this may also be possibly true for a random connection model.

### A. Expected Number of Isolated Nodes in an Asymptotically Infinite Network

In this subsection we analyze the expected number of isolated nodes in $\mathcal{G}\left(\mathcal{X}_{\frac{\log\rho+b}{C}}, g, A_{\frac{1}{r_\rho}}\right)$. For an arbitrary node in $\mathcal{G}\left(\mathcal{X}_{\frac{\log\rho+b}{C}}, g, A_{\frac{1}{r_\rho}}\right)$ at location $\boldsymbol{y}$, it can be shown that the probability that the node is isolated is given by [4]:

$$\Pr\left(I_{\boldsymbol{y}}=1\right)=e^{-\int_{A_{\frac{1}{r_\rho}}}\frac{\log\rho+b}{C}g(\|\boldsymbol{x}-\boldsymbol{y}\|)d\boldsymbol{x}} \tag{7}$$

where $I_{\boldsymbol{y}}$ is an indicator random variable: $I_{\boldsymbol{y}}=1$ if the node at $\boldsymbol{y}$ is isolated and $I_{\boldsymbol{y}}=0$ otherwise. Denote by $W$ the number of isolated nodes in an instance of $\mathcal{G}\left(\mathcal{X}_{\frac{\log\rho+b}{C}}, g, A_{\frac{1}{r_\rho}}\right)$. It then follows that the expected number of isolated nodes in $\mathcal{G}\left(\mathcal{X}_{\frac{\log\rho+b}{C}}, g, A_{\frac{1}{r_\rho}}\right)$ is given by

$$E\left(W\right)=\int_{A_{\frac{1}{r_\rho}}}\frac{\log\rho+b}{C}e^{-\int_{A_{\frac{1}{r_\rho}}}\frac{\log\rho+b}{C}g(\|\boldsymbol{x}-\boldsymbol{y}\|)d\boldsymbol{x}}d\boldsymbol{y} \tag{8}$$

On the basis of (8), the following theorem can be obtained.

*Theorem 1:* The expected number of isolated nodes in $\mathcal{G}\left(\mathcal{X}_{\frac{\log\rho+b}{C}}, g, A_{\frac{1}{r_\rho}}\right)$ is $\int_{A_{\frac{1}{r_\rho}}}\frac{\log\rho+b}{C}e^{-\int_{A_{\frac{1}{r_\rho}}}\frac{\log\rho+b}{C}g(\|\boldsymbol{x}-\boldsymbol{y}\|)d\boldsymbol{x}}d\boldsymbol{y}$. For $g$ satisfying both (1) and (4), the expected number of isolated nodes in $\mathcal{G}\left(\mathcal{X}_{\frac{\log\rho+b}{C}}, g, A_{\frac{1}{r_\rho}}\right)$ converges asymptotically to $e^{-b}$ as $\rho\to\infty$.

*Proof:* See Appendix I ■

*1) Impact of Boundary Effect on the Number of Isolated Nodes:* Before we proceed to the comparison of the expected number of isolated nodes in $\mathcal{G}\left(\mathcal{X}_{\frac{\log\rho+b}{C}}, g, A_{\frac{1}{r_\rho}}\right)$ and the expected number in its counterpart in an infinite network, we first examine the impact of boundary effect on the number of isolated nodes in $\mathcal{G}\left(\mathcal{X}_{\frac{\log\rho+b}{C}}, g, A_{\frac{1}{r_\rho}}\right)$. Boundary effect is a common concern in the analysis of network connectivity. The analysis of the impact of the boundary effect is done by comparing the number of isolated nodes in $\mathcal{G}\left(\mathcal{X}_{\frac{\log\rho+b}{C}}, g, A_{\frac{1}{r_\rho}}\right)$ and the number in a network with nodes Poissonly distributed on a torus $A^T_{\frac{1}{r_\rho}}\triangleq\left[-\frac{1}{2r_\rho},\frac{1}{2r_\rho}\right]^2$ with node density $\frac{\log\rho+b}{C}$ and where a pair of nodes separated by a *toroidal distance* $x^T$ [10, p. 13] are directly connected with probability $g\left(x^T\right)$, independent of the event that another distinct pair of nodes are directly connected. Denote the network on a torus by $\mathcal{G}^T\left(\mathcal{X}_{\frac{\log\rho+b}{C}}, g, A^T_{\frac{1}{r_\rho}}\right)$. The following lemma can be established.

*Lemma 1:* The expected number of isolated nodes in $\mathcal{G}^T\left(\mathcal{X}_{\frac{\log\rho+b}{C}}, g, A^T_{\frac{1}{r_\rho}}\right)$ is $\rho e^{-\int_{A_{\frac{1}{r_\rho}}}\frac{\log\rho+b}{C}g(\|\boldsymbol{x}\|)d\boldsymbol{x}}$. For $g$ satisfying both (1) and (4), the expected number of isolated nodes in $\mathcal{G}^T\left(\mathcal{X}_{\frac{\log\rho+b}{C}}, g, A_{\frac{1}{r_\rho}}\right)$ converges to $e^{-b}$ as $\rho\to\infty$.

*Proof:* See Appendix II ■

On the basis of Theorem 1 and Lemma 1, and using the coupling technique, the following lemma can be obtained.

*Lemma 2:* For $g$ satisfying both (1) and (4), the number of isolated nodes in $\mathcal{G}\left(\mathcal{X}_{\frac{\log\rho+b}{C}}, g, A_{\frac{1}{r_\rho}}\right)$ due to the boundary effect is a.a.s. $0$ as $\rho\to\infty$.

*Proof:* Comparing Theorem 1 and Lemma 1, it is noted that the expected numbers of isolated nodes on a torus and on a square respectively asymptotically converge to the same *non-zero finite constant* $e^{-b}$ as $\rho\to\infty$. Now we use the coupling technique [2] to construct the connection between $W$ and $W^T$, the number of isolated nodes in the corresponding instance

of $\mathcal{G}^T\left(\mathcal{X}_{\frac{\log\rho+b}{C}}, g, A_{\frac{1}{r_\rho}}\right)$. Consider an instance of $\mathcal{G}^T\left(\mathcal{X}_{\frac{\log\rho+b}{C}}, g, A^T_{\frac{1}{r_\rho}}\right)$. The number of isolated nodes in that network is $W^T$, which depends on $\rho$. Remove each connection of the above network with probability $1-\frac{g(x)}{g(x^T)}$, independent of the event that another connection is removed, where $x$ is the Euclidean distance between the two endpoints of the connection and $x^T$ is the corresponding toroidal distance. Due to $x^T \le x$ (see (40) in Appendix II) and the non-increasing property of $g$, $0 \le 1-\frac{g(x)}{g(x^T)} \le 1$. Further note that only connections between nodes near the boundary with $x^T < x$ will be affected, i.e. when $x = x^T$ the removal probability is zero. Denote the number of *newly* appearing isolated nodes by $W^E$. $W^E$ has the meaning of being *the number of isolated nodes due to the boundary effect*. It is straightforward to show that $W^E$ is a *non-negative random integer*, depending on $\rho$. Further, such a connection removal process results a random network with nodes Poissonly distributed with density $\frac{\log\rho+b}{C}$ where a pair of nodes separated by a *Euclidean* distance $x$ are directly connected with probability $g(x)$, i.e. a random network on a square with the boundary effect included. The following equation results as a consequence of the above discussion:

$$W = W^E + W^T$$

Using Theorem 1, Lemma 1 and the above equation, it can be shown that

$$\lim_{\rho\to\infty} E\left(W^E\right) = \lim_{\rho\to\infty} E\left(W - W^T\right) = 0$$

Due to the non-negativity of $W^E$:

$$\lim_{\rho\to\infty} \Pr\left(W^E = 0\right) = 1$$

■

*Remark 1:* Note that for $g$ not satisfying (4), $E(W)$ and $E\left(W^T\right)$ are not necessarily convergent as $\rho\to\infty$. Particularly using the same procedure in Appendix I and II (see also (14) in Section IV-C below), it can be shown that when $g(x) = \omega_x\left(\frac{1}{x^2\log^2 x}\right)$, both $\lim_{\rho\to\infty} E(W)$ and $\lim_{\rho\to\infty} E\left(W^T\right)$ are unbounded. When $g(x) = \Theta_x\left(\frac{1}{x^2\log^2 x}\right)$, $\lim_{\rho\to\infty} E(W)$ and $\lim_{\rho\to\infty} E\left(W^T\right)$ start to depend on the asymptotic behavior of $g$ and is only convergent when $\lim_{x\to\infty} g(x)\, x^2 \log^2 x = a$, where $0 < a < \infty$ is a positive constant. In that case, it can be shown that $\lim_{\rho\to\infty} E(W)$ and $\lim_{\rho\to\infty} E\left(W^T\right)$ converge to $e^{-b+\frac{4\pi}{C}a}$. For $\lim_{\rho\to\infty} E\left(W^T\right)$ the above result can be established by first choosing a small positive constant $\triangle\varepsilon$ and then letting $\rho$ be sufficiently large such that $D\left(\mathbf{0}, \frac{1}{2}r_\rho^{-1-\triangle\varepsilon}\right)$ contains $A_{\frac{1}{r_\rho}}$, where $D(\boldsymbol{x}, r)$ denotes a disk centered at $\boldsymbol{x}$ and with a radius $r$. An upper and lower bound on $E\left(W^T\right)$ can then be established by noting that

$$\begin{aligned}
& \lim_{\rho\to\infty} \rho e^{-\int_{D\left(\mathbf{0},\frac{1}{2}r_\rho^{-1-\triangle\varepsilon}\right)} \frac{\log\rho+b}{C} g(\|\boldsymbol{x}\|)d\boldsymbol{x}} \\
\le\ & \lim_{\rho\to\infty} E\left(W^T\right) = \rho e^{-\int_{A_{\frac{1}{r_\rho}}} \frac{\log\rho+b}{C} g(\|\boldsymbol{x}\|)d\boldsymbol{x}} \\
\le\ & \lim_{\rho\to\infty} \rho e^{-\int_{D\left(\mathbf{0},\frac{1}{2}r_\rho^{-1}\right)} \frac{\log\rho+b}{C} g(\|\boldsymbol{x}\|)d\boldsymbol{x}}
\end{aligned}$$

Following the exactly same procedure as that in (45) and (46) (in Appendix II) and finally letting $\triangle\varepsilon\to 0$, the result for $\lim_{\rho\to\infty} E\left(W^T\right)$ can be obtained. The result for $\lim_{\rho\to\infty} E(W)$ can be obtained following a similar procedure as that in Appendix I.

### *B. The Number of Isolated Nodes in a Region $A_{\frac{1}{r_\rho}}$ of an Infinite Network with Node Density $\frac{\log\rho+b}{C}$*

In this subsection, we consider the number of isolated nodes in the counterpart of $\mathcal{G}\left(\mathcal{X}_{\frac{\log\rho+b}{C}}, g, A_{\frac{1}{r_\rho}}\right)$ in an infinite network. Specifically, for a meaningful comparison with the number of isolated nodes in $\mathcal{G}\left(\mathcal{X}_{\frac{\log\rho+b}{C}}, g, A_{\frac{1}{r_\rho}}\right)$, we consider the number of isolated nodes, denoted by $W^\infty$ (with superscript $^\infty$ marking the parameter in an infinite network), in a square $A_{\frac{1}{r_\rho}}$ of an infinite network on $\Re^2$ with Poissonly distributed node at density $\frac{\log\rho+b}{C}$. Denote the infinite network by $\mathcal{G}\left(\mathcal{X}_{\frac{\log\rho+b}{C}}, g, \Re^2\right)$. For $g$ satisfying (2), a randomly chosen node in $\mathcal{G}\left(\mathcal{X}_{\frac{\log\rho+b}{C}}, g, \Re^2\right)$, at location $\boldsymbol{y}\in A_{\frac{1}{r_\rho}}$, is isolated with probability

$$\Pr\left(I_{\boldsymbol{y}}^\infty = 1\right) = e^{-\int_{\Re^2} \frac{\log\rho+b}{C} g(\|\boldsymbol{x}-\boldsymbol{y}\|)d\boldsymbol{x}} = \frac{1}{\rho}e^{-b} \tag{9}$$

where (2) is used in the above equation. Therefore

$$E\left(W^\infty\right) = \int_{A_{\frac{1}{r_\rho}}} \frac{\log\rho+b}{C} \times \frac{1}{\rho}e^{-b} d\boldsymbol{y}$$

$$
\begin{aligned}
&= \frac{\log\rho + b}{C} \times \frac{1}{\rho} e^{-b} \times \left(\frac{1}{r_\rho}\right)^2 \\
&= e^{-b}
\end{aligned}
\tag{10}
$$

The last line follows by (5).

The above result is summarized in the following lemma:

*Lemma 3:* For $g$ satisfying (2), the expected number of isolated nodes in a region $A_{\frac{1}{r_\rho}}$ of $\mathcal{G}\left(\mathcal{X}_{\frac{\log\rho+b}{C}}, g, \Re^2\right)$ is $e^{-b}$.

### *C. A Comparison of the Expected Number of Isolated Nodes in* $\mathcal{G}\left(\mathcal{X}_{\frac{\log\rho+b}{C}}, g, A_{\frac{1}{r_\rho}}\right)$ *and In Its Counterpart in An Infinite Network*

Comparing Theorem 1 and Lemma 3, we note that:

1) The expected number of isolated nodes in $\mathcal{G}\left(\mathcal{X}_{\frac{\log\rho+b}{C}}, g, A_{\frac{1}{r_\rho}}\right)$ only *converges asymptotically* to $e^{-b}$ as $\rho \to \infty$ whereas the expected number of isolated nodes in an area of the same size in $\mathcal{G}\left(\mathcal{X}_{\frac{\log\rho+b}{C}}, g, \Re^2\right)$ *is always* $e^{-b}$ no matter which value $\rho$ takes.
2) The expected number of isolated nodes in $\mathcal{G}\left(\mathcal{X}_{\frac{\log\rho+b}{C}}, g, A_{\frac{1}{r_\rho}}\right)$ converges asymptotically to $e^{-b}$ for $g$ *satisfying both* (1) *and* (4) whereas the expected number of isolated nodes in an area of the same size in $\mathcal{G}\left(\mathcal{X}_{\frac{\log\rho+b}{C}}, g, \Re^2\right)$ is $e^{-b}$ for $g$ *satisfying* (2) *only*.

In the following we examine the reason behind the differences.

Using (7), (8), (9) and (10), it can be shown that

$$
\begin{aligned}
&\frac{E(W)}{E(W^\infty)} \\
=&e^b \int_{A_{\frac{1}{r_\rho}}} \frac{\log\rho+b}{C} e^{-\int_{A_{\frac{1}{r_\rho}}} \frac{\log\rho+b}{C} g(\|\boldsymbol{x}-\boldsymbol{y}\|)d\boldsymbol{x}} d\boldsymbol{y} \\
=&e^b \int_{A_{\frac{1}{r_\rho}}} \frac{\log\rho+b}{C} \exp\left(-\int_{\Re^2} \frac{\log\rho+b}{C} g(\|\boldsymbol{x}-\boldsymbol{y}\|)\, d\boldsymbol{x}\right. \\
&\times \left.\int_{\Re^2\setminus A_{\frac{1}{r_\rho}}} \frac{\log\rho+b}{C} g(\|\boldsymbol{x}-\boldsymbol{y}\|)\, d\boldsymbol{x}\right) d\boldsymbol{y} \\
=&\int_{A_{\frac{1}{r_\rho}}} \frac{\log\rho+b}{C\rho} e^{\int_{\Re^2\setminus A_{\frac{1}{r_\rho}}} \frac{\log\rho+b}{C} g(\|\boldsymbol{x}-\boldsymbol{y}\|)d\boldsymbol{x}} d\boldsymbol{y}
\end{aligned}
\tag{11}
$$

It is trivial to show that the value in (11) is always greater than 1 for $g$ with infinite support. That is, for any $g$ with infinite support, the expected number of isolated nodes in $\mathcal{G}\left(\mathcal{X}_{\frac{\log\rho+b}{C}}, g, A_{\frac{1}{r_\rho}}\right)$ is strictly larger than the expected number of isolated nodes in an area $A_{\frac{1}{r_\rho}}$ of $\mathcal{G}\left(\mathcal{X}_{\frac{\log\rho+b}{C}}, g, \Re^2\right)$. Further, it can be shown that the value in (11) accounts for the cumulative effect of nodes outside $A_{\frac{1}{r_\rho}}$ in $\mathcal{G}\left(\mathcal{X}_{\frac{\log\rho+b}{C}}, g, \Re^2\right)$ and the associated connections between these nodes and nodes inside $A_{\frac{1}{r_\rho}}$ on decreasing the expected number of isolated nodes in $A_{\frac{1}{r_\rho}}$ respectively. Because $\mathcal{G}\left(\mathcal{X}_{\frac{\log\rho+b}{C}}, g, A_{\frac{1}{r_\rho}}\right)$ can be obtained from $\mathcal{G}\left(\mathcal{X}_{\frac{\log\rho+b}{C}}, g, \Re^2\right)$ by removing all these nodes and associated connections outside an area of $A_{\frac{1}{r_\rho}}$ in $\mathcal{G}\left(\mathcal{X}_{\frac{\log\rho+b}{C}}, g, \Re^2\right)$, we term the this distinction *the truncation effect*. Theorem 1 and Lemma 3 shows that when $g$ satisfies both (1) and (4) (i.e. $g$ has to decrease fast enough), the impact of the truncation effect on isolated nodes becomes vanishingly small as $\rho \to \infty$.

Based on the above discussion, the following theorem can be established:

*Theorem 2:* For $g$ satisfying (2), the expected number of isolated nodes in an area of $A_{\frac{1}{r_\rho}}$ in $\mathcal{G}\left(\mathcal{X}_{\frac{\log\rho+b}{C}}, g, \Re^2\right)$ is $e^{-b}$. Removing all nodes of $\mathcal{G}\left(\mathcal{X}_{\frac{\log\rho+b}{C}}, g, \Re^2\right)$ outside $A_{\frac{1}{r_\rho}}$ and the associated connections, there results $\mathcal{G}\left(\mathcal{X}_{\frac{\log\rho+b}{C}}, g, A_{\frac{1}{r_\rho}}\right)$. The expected number of isolated nodes in $\mathcal{G}\left(\mathcal{X}_{\frac{\log\rho+b}{C}}, g, A_{\frac{1}{r_\rho}}\right)$ converges to $e^{-b}$ if $g$ satisfies both (1) and (4). The more restrictive requirement on $g$ is a sufficient condition for the impact of the *truncation effect* associated with the above removal operations on the number of isolated nodes in $\mathcal{G}\left(\mathcal{X}_{\frac{\log\rho+b}{C}}, g, A_{\frac{1}{r_\rho}}\right)$ to be vanishingly small as $\rho \to \infty$.

In the following, we show that the more restrictive requirement on $g$ in (4) (compared with (1) and (2)) is also necessary for the impact of the truncation effect to become vanishingly small as $\rho \to \infty$. Specifically, consider the case when (4) is not satisfied. Let

$$f(x) \triangleq g(x)\, x^2 \log^2 x \tag{12}$$

Condition (4) not being satisfied means

$$\lim_{x\to\infty} f(x) \neq 0 \tag{13}$$

i.e. $\lim_{x\to\infty} f(x)$ may equal to a positive constant, $\infty$, or does not exist (e.g. $f(x)$ is a periodic function of $x$).

It can be shown that (following the equation, detailed explanations are given and see also (42) in Appendix II)

$$\begin{aligned}
& \lim_{\rho\to\infty} E(W) \\
\geq & \lim_{\rho\to\infty} E\left(W^T\right) \\
= & \lim_{\rho\to\infty} \rho e^{-\int_{A_{\frac{1}{r_\rho}}} \frac{\log\rho+b}{C} g(\|\boldsymbol{x}\|)d\boldsymbol{x}} \\
\geq & \lim_{\rho\to\infty} \rho e^{-\int_{D\left(\mathbf{0},\frac{1}{2}r_\rho^{-1}\right)} \frac{\log\rho+b}{C} g(\|\boldsymbol{x}\|)d\boldsymbol{x}} \\
= & e^{-b} \lim_{\rho\to\infty} e^{\int_{\Re^2\setminus D\left(\mathbf{0},\frac{1}{2}r_\rho^{-1}\right)} \frac{\log\rho+b}{C} g(\|\boldsymbol{x}\|)d\boldsymbol{x}} \\
= & e^{-b+\frac{4\pi}{C}\lim_{x\to\infty} f(x)}
\end{aligned} \tag{14}$$

where the last step results because of the following equation:

$$\begin{aligned}
& \int_{\Re^2\setminus D\left(\mathbf{0},\frac{1}{2}r_\rho^{-1}\right)} \frac{\log\rho+b}{C} g(\|\boldsymbol{x}\|)\, d\boldsymbol{x} \\
= & \lim_{\rho\to\infty} \int_{\frac{1}{2}r_\rho^{-1}}^{\infty} \frac{\log\rho+b}{C} 2\pi x g(x)\, dx \\
= & \lim_{\rho\to\infty} \frac{\frac{\pi}{2} r_\rho^{-4} g\left(\frac{1}{2}r_\rho^{-1}\right) \frac{\log\rho+b-1}{C\rho^2}}{\frac{C}{\rho(\log\rho+b)^2}} \\
= & \lim_{\rho\to\infty} \frac{\pi}{2C} (\log\rho+b)^2 r_\rho^{-2} g\left(\frac{1}{2}r_\rho^{-1}\right) \\
= & \lim_{\rho\to\infty} \frac{\pi}{2C} (\log\rho+b)^2 r_\rho^{-2} \frac{f\left(\frac{1}{2}r_\rho^{-1}\right)}{\frac{1}{4}r_\rho^{-2}\log^2\left(\frac{1}{2}r_\rho^{-1}\right)} \\
= & \lim_{\rho\to\infty} \frac{2\pi(\log\rho+b)^2 f\left(\frac{1}{2}r_\rho^{-1}\right)}{C\left(\log\frac{1}{2} - \frac{1}{2}\log(\log\rho+b) + \frac{1}{2}\log\rho + \frac{1}{2}\log C\right)^2} \\
= & \frac{4\pi}{C} \lim_{\rho\to\infty} f\left(\frac{1}{2}r_\rho^{-1}\right) \\
= & \frac{4\pi}{C} \lim_{x\to\infty} f(x)
\end{aligned}$$

where in the second step, L'Hôpital's rule with $\frac{C}{\log\rho+b}$ being the denominator and $\int_{\frac{1}{2}r_\rho^{-1}}^{\infty} 2\pi x g(x)\, dx$ being the numerator is used; in the third step, (12) is used.

*Remark 2:* Equation (14) shows also that $\lim_{\rho\to\infty} E\left(W^T\right) \geq e^{-b+\frac{4\pi}{C}\lim_{x\to\infty} f(x)}$ where $E\left(W^T\right)$ is the expected number of isolated nodes on a torus, which does not include the contribution of the boundary effect on the number of isolated nodes. Note also that the expected number of isolated nodes in an area of $A_{\frac{1}{r_\rho}}$ in $\mathcal{G}\left(\mathcal{X}_{\frac{\log\rho+b}{C}}, g, \Re^2\right)$ is $e^{-b}$. Therefore the term $e^{\frac{4\pi}{C}\lim_{x\to\infty} f(x)}$ is entirely attributable to the truncation effect.

Note that $f(x)$ is a non-negative function for $x > 1$. It is obvious from (14) that *unless* $\lim_{x\to\infty} f(x) = 0$, i.e. (4) is satisfied, the expected number of isolated node in $\mathcal{G}\left(\mathcal{X}_{\frac{\log\rho+b}{C}}, g, A_{\frac{1}{r_\rho}}\right)$ will be larger than the expected number of isolated nodes in an area of $A_{\frac{1}{r_\rho}}$ in $\mathcal{G}\left(\mathcal{X}_{\frac{\log\rho+b}{C}}, g, \Re^2\right)$. That is, the impact of the *truncation effect* on the number of isolated nodes in $\mathcal{G}\left(\mathcal{X}_{\frac{\log\rho+b}{C}}, g, A_{\frac{1}{r_\rho}}\right)$ will *not be* vanishingly small as $\rho \to \infty$. In particular, it can be shown that for $g(x) = \Theta_x\left(\frac{1}{x^2\log^2 x}\right)$, the impact of the

truncation effect is non-negligible or even dominant in determining the number of isolated nodes in $\mathcal{G}\left(\mathcal{X}_{\frac{\log\rho+b}{C}}, g, A_{\frac{1}{r_\rho}}\right)$. Using (14), it can also be shown that for $g(x)=\omega_x\left(\frac{1}{x^2\log^2 x}\right)$, $\lim_{\rho\to\infty} E(W)$ is unbounded, i.e. connectivity cannot be achieved for $g(x)=\omega_x\left(\frac{1}{x^2\log^2 x}\right)$ even if (1) and (2) are satisfied.

The above discussion leads to the following conclusion:

*Theorem 3:* The more restrictive requirement on $g$ that it satisfies (4) is a necessary condition for the impact of the *truncation effect* on the number of isolated nodes in $\mathcal{G}\left(\mathcal{X}_{\frac{\log\rho+b}{C}}, g, A_{\frac{1}{r_\rho}}\right)$ to be vanishingly small as $\rho\to\infty$. Further for $g(x)=\Theta_x\left(\frac{1}{x^2\log^2 x}\right)$, the impact of the truncation effect is non-negligible or even dominant in determining the number of isolated nodes in $\mathcal{G}\left(\mathcal{X}_{\frac{\log\rho+b}{C}}, g, A_{\frac{1}{r_\rho}}\right)$; and for $g(x)=\omega_x\left(\frac{1}{x^2\log^2 x}\right)$, the truncation effect is the dominant factor in determining the number of isolated nodes in $\mathcal{G}\left(\mathcal{X}_{\frac{\log\rho+b}{C}}, g, A_{\frac{1}{r_\rho}}\right)$.

Noting that the number of isolated nodes in a network is a non-negative integer, the following result can be obtained as an easy consequence of Theorem 2 (see also [32]). Notice that in formulating this result, we drop the assumption that $b$, originally introduced in (5), is a constant, and allow it instead to be $\rho$-dependent.

*Corollary 1:* For $g$ satisfying both (1) and (4), a necessary condition for $\mathcal{G}\left(\mathcal{X}_{\frac{\log\rho+b}{C}}, g, A_{\frac{1}{r_\rho}}\right)$ to be *a.a.s.* (as $\rho\to\infty$) connected is $b\to\infty$.

*Remark 3:* As pointed out in [2, p. 151], the three requirements on $g$ in the random connection model, i.e. rotational invariance, non-increasing monotonicity and integral boundedness, are not equally important. Particularly, rotational invariance and non-increasing monotonicity are required only to simply the analysis such that "the notation and formulae will be somewhat simpler". Similarly, we expect the results obtained in this section and in the next section requiring non-increasing monotonicity in (1) are also valid when the condition in (1) is removed. These however require more complicated handling of $g(x)$, particularly when $x$ is sufficiently large.

## V. Vanishing of Components of Finite Order

In this section we consider the events of the asymptotic vanishing of components of fixed and finite order $k>1$ in the infinite network $\mathcal{G}\left(\mathcal{X}_{\frac{\log\rho+b}{C}}, g, \Re^2\right)$ and in $\mathcal{G}\left(\mathcal{X}_{\frac{\log\rho+b}{C}}, g, A_{\frac{1}{r_\rho}}\right)$ respectively as $\rho\to\infty$.

In [2, Theorem 6.4] it was shown that as $\rho\to\infty$ (and $\frac{\log\rho+b}{C}\to\infty$) the probability for a node to be isolated given that its component is finite converges to 1. In other words, as $\rho\to\infty$ a.a.s. $\mathcal{G}\left(\mathcal{X}_{\frac{\log\rho+b}{C}}, g, \Re^2\right)$ has only isolated nodes and components of infinite order, and components of fixed and finite order $k>1$ asymptotically vanish. In the following we show that due to the truncation effect, the above result obtained in $\mathcal{G}\left(\mathcal{X}_{\frac{\log\rho+b}{C}}, g, \Re^2\right)$ does *not* carry over to the conclusion that as $\rho\to\infty$ a.a.s. $\mathcal{G}\left(\mathcal{X}_{\frac{\log\rho+b}{C}}, g, A_{\frac{1}{r_\rho}}\right)$ has only isolated nodes and infinite components too, without further analysis on the impact of the truncation effect**.** Specifically, an infinite component in $\mathcal{G}\left(\mathcal{X}_{\frac{\log\rho+b}{C}}, g, \Re^2\right)$ may *possibly* consist of components of extremely large order, components of fixed and finite order $k>1$ and isolated nodes involving nodes and connections entirely contained inside $A_{\frac{1}{r_\rho}}$, where these components are only connected to each other via nodes and connections outside $A_{\frac{1}{r_\rho}}$. Note that for any finite $\rho$, almost surely there is no infinite component in $\mathcal{G}\left(\mathcal{X}_{\frac{\log\rho+b}{C}}, g, A_{\frac{1}{r_\rho}}\right)$. Therefore we use the term *component of extremely large order* to refer to a component whose order may become asymptotically infinite as $\rho\to\infty$. As the nodes and associated connections outside $A_{\frac{1}{r_\rho}}$ are removed, the infinite component in $\Re^2$ may *possibly* leave components of extremely large order, components of finite order $k>1$ and isolated nodes in $A_{\frac{1}{r_\rho}}$. As such, vanishing of components of finite order $k>1$ in $\mathcal{G}\left(\mathcal{X}_{\frac{\log\rho+b}{C}}, g, \Re^2\right)$ as $\rho\to\infty$ does not *necessarily* carry the conclusion that components of finite order $k>1$ in $\mathcal{G}\left(\mathcal{X}_{\frac{\log\rho+b}{C}}, g, A_{\frac{1}{r_\rho}}\right)$ also vanish as $\rho\to\infty$, even when $A_{\frac{1}{r_\rho}}$ approaches $\Re^2$ as $\rho\to\infty$. An example is illustrated in Fig. 1.

We further point out that many other topologies, particularly under a random connection model where even a pair of nodes separated by a large distance may have a non-zero probability to be directly connected, can be drawn for an infinite component in $\Re^2$, where after removing all nodes and associated connections of the infinite component outside $A_{\frac{1}{r_\rho}}$, the infinite component leaves components of finite order $k>1$ inside $A_{\frac{1}{r_\rho}}$, even when $A_{\frac{1}{r_\rho}}$ grows as $\rho\to\infty$. We emphasize that we are not hinting that the topology of the infinite component shown in Fig. 1 is likely to occur in $\mathcal{G}\left(\mathcal{X}_{\frac{\log\rho+b}{C}}, g, \Re^2\right)$ as $\rho\to\infty$, but neither can such a possibility be precluded using [2, Theorem 6.4]. Therefore a conclusion cannot be drawn straightforwardly from [2, Theorem 6.4] that a.a.s. components of finite order $k>1$ in $\mathcal{G}\left(\mathcal{X}_{\frac{\log\rho+b}{C}}, g, A_{\frac{1}{r_\rho}}\right)$ vanish as $\rho\to\infty$. Instead some non-trivial analysis is required to establish such a conclusion in $\mathcal{G}\left(\mathcal{X}_{\frac{\log\rho+b}{C}}, g, A_{\frac{1}{r_\rho}}\right)$.

We present such a result for the vanishing of components of finite order $k>1$ in $\mathcal{G}\left(\mathcal{X}_{\frac{\log\rho+b}{C}}, g, A_{\frac{1}{r_\rho}}\right)$ as $\rho\to\infty$ to fill this theoretical gap:

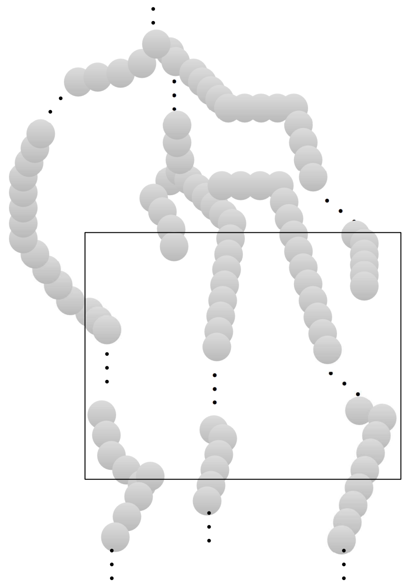

Figure 1: An illustration that an infinite component in $\Re^2$ may leave components of extremely large order, components of finite order $k > 1$ and isolated nodes in a finite (or asymptotically infinite) region in $\Re^2$ when nodes and connections outside the finite (asymptotically infinite) region is removed. The figure uses the unit disk connection model as a special case for easy illustration. Each ball has a radius of half of the transmission range and is centered at a node. Two adjacent balls overlap iff the associated nodes are directly connected. The figure shows an infinite component with nodes organized in a tree structure. The square area represents the finite (asymptotically infinite) region. Even as the square grows to include more and more nodes of the infinite component, it is still possible for the square to have components of finite order $k > 1$ when nodes and connections outside the square are removed.

*Theorem 4:* For $g$ satisfying (1) and (4), a.a.s. there is no component of finite order $k > 1$ in $\mathcal{G}\left(\mathcal{X}_{\frac{\log \rho + b}{C}}, g, A_{\frac{1}{r_\rho}}\right)$.

*Proof:* See Appendix III. ■

*Remark 4:* Theorem 4 gives a sufficient condition on $g$ required for the number of components of fixed and finite order $k > 1$ in $\mathcal{G}\left(\mathcal{X}_{\frac{\log \rho + b}{C}}, g, A_{\frac{1}{r_\rho}}\right)$ to be vanishingly small as $\rho \to \infty$. It is also interesting to obtain a necessary condition on $g$ required for the number of components of fixed and finite order $k > 1$ in $\mathcal{G}\left(\mathcal{X}_{\frac{\log \rho + b}{C}}, g, A_{\frac{1}{r_\rho}}\right)$ to be vanishingly small. The technique used in the proof of Theorem 4 however cannot answer the above question on a necessary condition on $g$. More specifically, denote by $\xi_k$ the (random) number of components of order $k$ in an instance of $\mathcal{G}\left(\mathcal{X}_\lambda, g, A_{\frac{1}{r_\rho}}\right)$ and let $M$ be an arbitrarily large positive integer $M$. The proof of Theorem 4 is based on an analysis of $E\left(\sum_{k=2}^{M} \xi_k\right)$. By showing that $\lim_{\rho\to\infty} E\left(\sum_{k=2}^{M} \xi_k\right) = 0$, it follows that $\lim_{\rho\to\infty} \Pr\left(\sum_{k=2}^{M} \xi_k = 0\right) = 1$. However $\lim_{\rho\to\infty} E\left(\sum_{k=2}^{M} \xi_k\right) = 0$ is only a sufficient condition for $\lim_{\rho\to\infty} \Pr\left(\sum_{k=2}^{M} \xi_k = 0\right) = 1$, *not* a necessary condition. It would be interesting to develop a technique to obtain a tight necessary condition on $g$ required for the number of components of fixed and finite order $k > 1$ in $\mathcal{G}\left(\mathcal{X}_{\frac{\log \rho + b}{C}}, g, A_{\frac{1}{r_\rho}}\right)$ to be vanishingly small.

## VI. Conclusion

In this paper, we discussed the connectivity of several network models including the widely used dense network model $\mathcal{G}\left(\mathcal{X}_\rho, g_{r_\rho}, A\right)$, extended network model $\mathcal{G}\left(\mathcal{X}_1, g_{\sqrt{\frac{\log \rho + b}{C}}}, A_{\sqrt{\rho}}\right)$ and infinite network model $\mathcal{G}\left(\mathcal{X}_\rho, g, \Re^2\right)$. Using the scaling and coupling technique, it is shown that the dense network model and the extended network model are equivalent in their connectivity properties and they are also equivalent to the network model $\mathcal{G}\left(\mathcal{X}_{\frac{\log \rho + b}{C}}, g, A_{\frac{1}{r_\rho}}\right)$, which can be obtained from the infinite network model $\mathcal{G}\left(\mathcal{X}_{\frac{\log \rho + b}{C}}, g, \Re^2\right)$ by removing all nodes and associated connections outside the area $A_{\frac{1}{r_\rho}}$ of $\mathcal{G}\left(\mathcal{X}_\rho, g, \Re^2\right)$. Define the effect associated with the above removal operation as the truncation effect. A prerequisite for any (asymptotic) conclusion obtained in the infinite network model to be applicable to the dense and extended network models is that the impact of the truncation effect must be vanishingly small on the parameter concerned as $\rho \to \infty$ - a conclusion that often needs non-trivial analysis to establish. We then conducted two case studies using a random connection model, on the expected number of isolated nodes and on the vanishing of components of fixed and finite order $k > 1$ respectively, with a

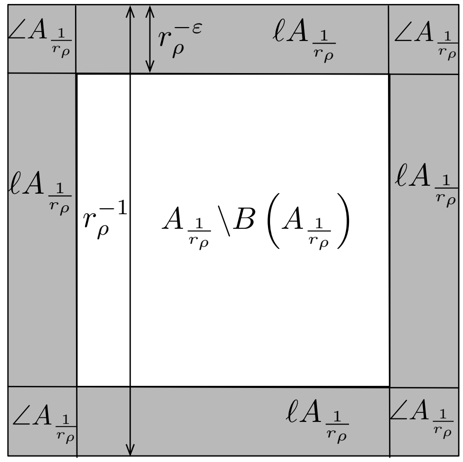


Figure 2: An Illustration of the boundary areas of $A_{\frac{1}{r_\rho}}$. The areas $\angle A_{\frac{1}{r_\rho}}$, $\ell A_{\frac{1}{r_\rho}}$ are self-explanatory and $B\left(A_{\frac{1}{r_\rho}}\right)$ is the shaded area in the figure.

focus on examining the impact of the truncation effect and showed that the connection function $g$ has to decrease sufficiently fast in order for the truncation effect to have a vanishingly small impact.

In the first case study, we showed that for $g$ satisfying both (1) and (4), the impact of the truncation effect on the number of isolated nodes in $\mathcal{G}\left(\mathcal{X}_{\frac{\log\rho+b}{C}}, g, A_{\frac{1}{r_\rho}}\right)$ is vanishingly small as $\rho \to \infty$. However for $g$ satisfying (1) and (2) only, the impact of the truncation effect on the number of isolated nodes in $\mathcal{G}\left(\mathcal{X}_{\frac{\log\rho+b}{C}}, g, A_{\frac{1}{r_\rho}}\right)$ is non-negligible and may even be the dominant factor in determining the number of isolated nodes.

In the second case study, we first showed using an example that due to the truncation effect, asymptotic vanishing of components of fixed and finite order $k > 1$ in an infinite network does not carry over straightforwardly to the conclusion that components of fixed and finite order $k > 1$ also vanish asymptotically in the dense and extended networks. Then to fill this theoretical gap, a result is presented on the asymptotic vanishing of components of finite order $k > 1$ in the dense and extended network models under a random connection model.

Some interesting results useful for the analysis of connectivity under a random connection model in the dense and extended networks were also established. These include the expected number of isolated nodes, which resulted in a necessary condition for a dense (or extended) network to be connected, the vanishingly small impact of the boundary effect on the number of isolated nodes, and the asymptotic vanishing of components of finite order $k > 1$.

Many results in the paper were given in the form of *sufficient* conditions on the connection function $g$ required for the impact of the truncation effect to be vanishingly small. It will be interesting and important to examine *necessary* conditions on $g$ required for the impact of the truncation effect to be vanishingly small.

## APPENDIX I PROOF OF THEOREM 1

In this Appendix, we give a proof of Theorem 1.

We analyze $E(W)$ as $\rho \to \infty$. Denote by $D\left(\boldsymbol{y}, r_\rho^{-\varepsilon}\right)$ a disk centered at $\boldsymbol{y}$ and with a radius $r_\rho^{-\varepsilon}$, where $\varepsilon$ is a small positive constant and $\varepsilon < \frac{1}{4}$. Denote by $B\left(A_{\frac{1}{r_\rho}}\right) \subset A_{\frac{1}{r_\rho}}$ an area within $r_\rho^{-\varepsilon}$ of the border of $A_{\frac{1}{r_\rho}}$; denote by $\ell A_{\frac{1}{r_\rho}} \subset A_{\frac{1}{r_\rho}}$ a rectangular area of size $r_\rho^{-\varepsilon} \times \left(r_\rho^{-1} - 2r_\rho^{-\varepsilon}\right)$ within $r_\rho^{-\varepsilon}$ of one side of $A_{\frac{1}{r_\rho}}$, away from the corners of $A_{\frac{1}{r_\rho}}$ by $r_\rho^{-\varepsilon}$, and there are four such areas; let $\angle A_{\frac{1}{r_\rho}} \subset A_{\frac{1}{r_\rho}}$ denote a square of size $r_\rho^{-\varepsilon} \times r_\rho^{-\varepsilon}$ at the four corners of $A_{\frac{1}{r_\rho}}$. Fig. 2 illustrates these areas.

It follows from (8) that

$$
\begin{aligned}
& \lim_{\rho\to\infty} E(W) \\
= & \lim_{\rho\to\infty} \int_{A_{\frac{1}{r_\rho}}} \frac{\log\rho+b}{C} e^{-\int_{A_{\frac{1}{r_\rho}}} \frac{\log\rho+b}{C} g(\|\boldsymbol{x}-\boldsymbol{y}\|)d\boldsymbol{x}} d\boldsymbol{y} \\
= & \lim_{\rho\to\infty} \rho r_\rho^2 \int_{A_{\frac{1}{r_\rho}} \backslash B\left(A_{\frac{1}{r_\rho}}\right)} e^{-\rho r_\rho^2 \int_{A_{\frac{1}{r_\rho}}} g(\|\boldsymbol{x}-\boldsymbol{y}\|)d\boldsymbol{x}} d\boldsymbol{y}
\end{aligned}
$$

$$+ \quad \lim_{\rho\to\infty} 4\rho r_\rho^2 \int_{\ell A_{\frac{1}{r_\rho}}} e^{-\rho r_\rho^2 \int_{A_{\frac{1}{r_\rho}}} g(\|\boldsymbol{x}-\boldsymbol{y}\|)d\boldsymbol{x}} d\boldsymbol{y}$$

$$+ \quad \lim_{\rho\to\infty} 4\rho r_\rho^2 \int_{\angle A_{\frac{1}{r_\rho}}} e^{-\rho r_\rho^2 \int_{A_{\frac{1}{r_\rho}}} g(\|\boldsymbol{x}-\boldsymbol{y}\|)d\boldsymbol{x}} d\boldsymbol{y} \tag{15}$$

The three summands in (15) represent respectively the expected number of isolated nodes in the central area $A_{\frac{1}{r_\rho}} \backslash B\left(A_{\frac{1}{r_\rho}}\right)$, in the boundary area along the four sides of $A_{\frac{1}{r_\rho}}$ and in the four corners of $A_{\frac{1}{r_\rho}}$. In the following analysis, we will show that for $g$ satisfying both (1) and (4), the first term approaches $e^{-b}$ as $\rho \to \infty$, and the second and the third terms approach $0$ as $\rho \to \infty$.

Consider the first summand in (15). Using the definition of $r_\rho$ in (5), first it can be shown that for any $\boldsymbol{y}$ and therefore $\boldsymbol{y} \in A_{\frac{1}{r_\rho}} \backslash B\left(A_{\frac{1}{r_\rho}}\right)$ (see Fig. 2 for the region $A_{\frac{1}{r_\rho}} \backslash B\left(A_{\frac{1}{r_\rho}}\right)$):

$$\begin{aligned}
& \lim_{\rho\to\infty} \rho e^{-\rho r_\rho^2 \int_{D\left(\boldsymbol{y}, r_\rho^{-\varepsilon}\right)} g(\|\boldsymbol{x}-\boldsymbol{y}\|)d\boldsymbol{x}} \\
= & \lim_{\rho\to\infty} \rho e^{-\rho r_\rho^2 \left(\int_{\Re^2} g(\|\boldsymbol{x}-\boldsymbol{y}\|)d\boldsymbol{x} - \int_{\Re^2 \backslash D\left(\boldsymbol{y}, r_\rho^{-\varepsilon}\right)} g(\|\boldsymbol{x}-\boldsymbol{y}\|)d\boldsymbol{x}\right)} \\
= & \lim_{\rho\to\infty} \rho e^{-\rho r_\rho^2 \left(C - \int_{\Re^2 \backslash D\left(\boldsymbol{y}, r_\rho^{-\varepsilon}\right)} g(\|\boldsymbol{x}-\boldsymbol{y}\|)d\boldsymbol{x}\right)} \\
= & \lim_{\rho\to\infty} e^{-b} e^{\rho r_\rho^2 \int_{\Re^2 \backslash D\left(\boldsymbol{y}, r_\rho^{-\varepsilon}\right)} g(\|\boldsymbol{x}-\boldsymbol{y}\|)d\boldsymbol{x}} \\
= & e^{-b} \lim_{\rho\to\infty} e^{\frac{\log\rho+b}{C} \int_{r_\rho^{-\varepsilon}}^{\infty} 2\pi r g(r) dr}
\end{aligned} \tag{16}$$

It can be shown further using (5) that (following the equation, detailed explanations are given):

$$\begin{aligned}
& \lim_{\rho\to\infty} \frac{\log\rho+b}{C} \int_{r_\rho^{-\varepsilon}}^{\infty} 2\pi r g(r)\, dr \\
= & \lim_{\rho\to\infty} \frac{\int_{r_\rho^{-\varepsilon}}^{\infty} 2\pi r g(r)\, dr}{\frac{C}{\log\rho+b}} \\
= & \lim_{\rho\to\infty} \frac{-2\pi r_\rho^{-\varepsilon} g\left(r_\rho^{-\varepsilon}\right)\left(-\frac{\varepsilon}{2} r_\rho^{-\varepsilon-2} \frac{1-(\log\rho+b)}{C\rho^2}\right)}{-\frac{C}{\rho(\log\rho+b)^2}} \\
= & \lim_{\rho\to\infty} \pi\varepsilon (\log\rho+b)^2 r_\rho^{-2\varepsilon-2} g\left(r_\rho^{-\varepsilon}\right) \frac{\log\rho+b-1}{C\rho} \\
= & \lim_{\rho\to\infty} \pi\varepsilon (\log\rho+b)^2 r_\rho^{-2\varepsilon} g\left(r_\rho^{-\varepsilon}\right) && (17) \\
= & \lim_{\rho\to\infty} \pi\varepsilon (\log\rho+b)^2 r_\rho^{-2\varepsilon} o_\rho\left(\frac{1}{r_\rho^{-2\varepsilon} \log^2\left(r_\rho^{-2\varepsilon}\right)}\right) && (18) \\
= & \lim_{\rho\to\infty} \Bigg(\pi\varepsilon (\log\rho+b)^2 \\
& o_\rho\left(\frac{1}{2\varepsilon^2 \left(\log\left(\log\rho+b\right) - \log C - \log\rho\right)^2}\right)\Bigg) \\
= & 0 && (19)
\end{aligned}$$

where L'Hôpital's rule is used in the second step of the above equation, and $g(x) = o_x\left(\frac{1}{x^2\log^2 x}\right)$ is used from (17) to (18). As a result of (16) and (19)

$$\lim_{\rho\to\infty} \rho e^{-\rho r_\rho^2 \int_{D\left(\boldsymbol{y}, r_\rho^{-\varepsilon}\right)} g(\|\boldsymbol{x}-\boldsymbol{y}\|)d\boldsymbol{x}} = e^{-b} \tag{20}$$

It follows that (see Fig. 2 for an illustration of the region $A_{\frac{1}{r_\rho}} \backslash B\left(A_{\frac{1}{r_\rho}}\right)$, which is unshaded in the figure.)

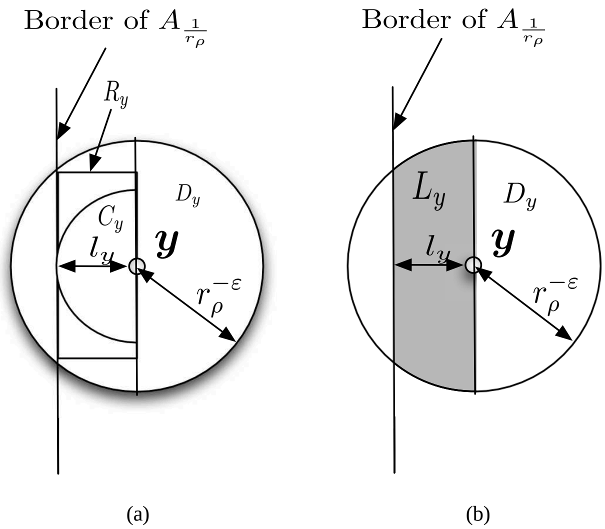


Figure 3: An illustration of the boundary area for $\boldsymbol{y} \in \ell A_{\frac{1}{r_\rho}}$. The figure is drawn for $\boldsymbol{y}$ located near the left border of $A_{\frac{1}{r_\rho}}$. The situations for $\boldsymbol{y}$ near the top, bottom and right borders of $A_{\frac{1}{r_\rho}}$ can be drawn analogously. $D\left(\boldsymbol{y}, r_\rho^{-\varepsilon}\right)$ is a disk centered at $\boldsymbol{y}$ and has a radius $r_\rho^{-\varepsilon}$. $l_y$ is the distance between $\boldsymbol{y}$ and the border of $A_{\frac{1}{r_\rho}}$. $D_y$ is a half disk centered at $\boldsymbol{y}$, with a radius $r_\rho^{-\varepsilon}$ and on the right side of $\boldsymbol{y}$. $C_y$ is a half disk centered at $\boldsymbol{y}$, with a radius $l_y$ and on the left side of $\boldsymbol{y}$. $R_y \subset A_{\frac{1}{r_\rho}} \cap D\left(\boldsymbol{y}, r_\rho^{-\varepsilon}\right)$ is a rectangle of $l_y \times 2\sqrt{r_\rho^{-2\varepsilon} - l_y^2}$ on the left side of $\boldsymbol{y}$. $L_y = \left(A_{\frac{1}{r_\rho}} \cap D\left(\boldsymbol{y}, r_\rho^{-\varepsilon}\right)\right) \backslash D_y$ is the shaded area in sub-figure b.

$$
\begin{aligned}
&\lim_{\rho\to\infty} \rho r_\rho^2 \int_{A_{\frac{1}{r_\rho}} \backslash B\left(A_{\frac{1}{r_\rho}}\right)} e^{-\rho r_\rho^2 \int_{A_{\frac{1}{r_\rho}}} g(\|\boldsymbol{x}-\boldsymbol{y}\|)d\boldsymbol{x}} d\boldsymbol{y} \\
\leq &\lim_{\rho\to\infty} \rho r_\rho^2 \int_{A_{\frac{1}{r_\rho}} \backslash B\left(A_{\frac{1}{r_\rho}}\right)} e^{-\rho r_\rho^2 \int_{D\left(\boldsymbol{y}, r_\rho^{-\varepsilon}\right)} g(\|\boldsymbol{x}-\boldsymbol{y}\|)d\boldsymbol{x}} d\boldsymbol{y} \\
= &\lim_{\rho\to\infty} \left(\rho e^{-\rho r_\rho^2 \int_{D\left(\mathbf{o}, r_\rho^{-\varepsilon}\right)} g(\|\boldsymbol{x}\|)d\boldsymbol{x}}\right) \left(r_\rho^2 \int_{A_{\frac{1}{r_\rho}} \backslash B\left(A_{\frac{1}{r_\rho}}\right)} d\boldsymbol{y}\right) \\
= &e^{-b}
\end{aligned}
$$

and

$$
\begin{aligned}
&\lim_{\rho\to\infty} \rho r_\rho^2 \int_{A_{\frac{1}{r_\rho}} \backslash B\left(A_{\frac{1}{r_\rho}}\right)} e^{-\rho r_\rho^2 \int_{A_{\frac{1}{r_\rho}}} g(\|\boldsymbol{x}-\boldsymbol{y}\|)d\boldsymbol{x}} d\boldsymbol{y} \\
\geq \quad &\lim_{\rho\to\infty} \rho r_\rho^2 \int_{A_{\frac{1}{r_\rho}} \backslash B\left(A_{\frac{1}{r_\rho}}\right)} e^{-\rho r_\rho^2 \int_{\Re^2} g(\|\boldsymbol{x}-\boldsymbol{y}\|)d\boldsymbol{x}} d\boldsymbol{y} \\
= \quad &e^{-b}
\end{aligned}
$$

Therefore

$$
\lim_{\rho\to\infty} \rho r_\rho^2 \int_{A_{\frac{1}{r_\rho}} / B\left(A_{\frac{1}{r_\rho}}\right)} e^{-\rho r_\rho^2 \int_{A_{\frac{1}{r_\rho}}} g(\|\boldsymbol{x}-\boldsymbol{y}\|)d\boldsymbol{x}} d\boldsymbol{y} = e^{-b} \tag{21}
$$

For the second term in (15), an illustration of the boundary area for $\boldsymbol{y} \in \ell A_{\frac{1}{r_\rho}}$ is shown in Fig. 3.

Define $L_y \triangleq \left(A_{\frac{1}{r_\rho}} \cap D\left(\boldsymbol{y}, r_\rho^{-\varepsilon}\right)\right) \backslash D_y$ (i.e. the shaded area in Fig. 3b). The symbols $D_y$, $C_y$, $l_y$ and $R_y$ are defined in Fig. 3. It can be shown that

$$
\begin{aligned}
&4\lim_{\rho\to\infty}\rho r_\rho^2\int_{\ell A_{\frac{1}{r_\rho}}} e^{-\rho r_\rho^2\int_{A_{\frac{1}{r_\rho}}} g(\|\boldsymbol{x}-\boldsymbol{y}\|)d\boldsymbol{x}} d\boldsymbol{y}\\
\leq&4\lim_{\rho\to\infty} r_\rho^2\int_{\ell A_{\frac{1}{r_\rho}}} \rho e^{-\rho r_\rho^2\int_{A_{\frac{1}{r_\rho}}\cap D\left(\boldsymbol{y},r_\rho^{-\varepsilon}\right)} g(\|\boldsymbol{x}-\boldsymbol{y}\|)d\boldsymbol{x}} d\boldsymbol{y}\\
=&4\lim_{\rho\to\infty} r_\rho^2\int_{\ell A_{\frac{1}{r_\rho}}} \rho e^{-\rho r_\rho^2\left(\int_{D_y} g(\|\boldsymbol{x}-\boldsymbol{y}\|)d\boldsymbol{x}+\int_{L_y} g(\|\boldsymbol{x}-\boldsymbol{y}\|)d\boldsymbol{x}\right)} d\boldsymbol{y}\\
=&4\lim_{\rho\to\infty}\left(\left(\rho^{\frac{1}{2}}e^{-\frac{1}{2}\rho r_\rho^2\int_{D\left(\mathbf{o},r_\rho^{-\varepsilon}\right)} g(\|\boldsymbol{x}\|)d\boldsymbol{x}}\right)\right.\\
&\left.\left(\rho^{\frac{1}{2}}r_\rho^2\int_{\ell A_{\frac{1}{r_\rho}}} e^{-\rho r_\rho^2\int_{L_y} g(\|\boldsymbol{x}-\boldsymbol{y}\|)d\boldsymbol{x}} d\boldsymbol{y}\right)\right)
\end{aligned}
\tag{22}
$$

For the first term $\rho^{\frac{1}{2}}e^{-\frac{1}{2}\rho r_\rho^2\int_{D\left(\mathbf{o},r_\rho^{-\varepsilon}\right)} g(\|\boldsymbol{x}\|)d\boldsymbol{x}}$ in (22), it can be shown that

$$
\begin{aligned}
&\lim_{\rho\to\infty}\rho^{\frac{1}{2}}e^{-\frac{1}{2}\rho r_\rho^2\int_{D\left(\mathbf{o},r_\rho^{-\varepsilon}\right)} g(\|\boldsymbol{x}\|)d\boldsymbol{x}}\\
=&\lim_{\rho\to\infty}\rho^{\frac{1}{2}}e^{-\frac{1}{2}\rho r_\rho^2\left(\int_{\Re^2} g(\|\boldsymbol{x}\|)d\boldsymbol{x}-\int_{\Re^2\backslash D\left(\mathbf{o},r_\rho^{-\varepsilon}\right)} g(\|\boldsymbol{x}\|)d\boldsymbol{x}\right)}\\
=&\lim_{\rho\to\infty}\rho^{\frac{1}{2}}e^{-\frac{1}{2}\rho r_\rho^2 C}e^{\frac{1}{2}\rho r_\rho^2\int_{\Re^2\backslash D\left(\mathbf{o},r_\rho^{-\varepsilon}\right)} g(\|\boldsymbol{x}\|)d\boldsymbol{x}}\\
=&e^{-\frac{b}{2}}
\end{aligned}
\tag{23}
$$

where (19) is used in reaching (23).

Let $\gamma$ be a positive constant and $\frac{1}{2}>\gamma>\frac{\varepsilon}{2}$. Let $\triangle$ be a positive constant such that

$$
\int_0^{\triangle} 2\pi x g\left(x\right)dx=\gamma 2C \tag{24}
$$

The existence of such a positive constant $\triangle$ can be shown by using (6) and noting that $2\gamma<1$. Using the non-increasing property of $g$, it can also be shown that $g\left(\triangle\right)>0$; otherwise it can be shown that $\int_0^{\triangle} 2\pi x g\left(x\right)dx=C$ which implies $\gamma=\frac{1}{2}$. This constitutes a contradiction with the requirement that $\frac{1}{2}>\gamma>\frac{\varepsilon}{2}$. Therefore $g\left(\triangle\right)>0$. In the following analysis, it is assumed that $\rho$ is sufficiently large such that $r_\rho^{-\varepsilon}\geq 2\triangle$.

For the second term in (22), it can be shown that

$$
\begin{aligned}
&\lim_{\rho\to\infty}\rho^{\frac{1}{2}}r_\rho^2\int_{\ell A_{\frac{1}{r_\rho}}} e^{-\rho r_\rho^2\int_{L_y} g(\|\boldsymbol{x}-\boldsymbol{y}\|)d\boldsymbol{x}} d\boldsymbol{y}\\
=&\lim_{\rho\to\infty}\left(\rho^{\frac{1}{2}}r_\rho^2\left(r_\rho^{-1}-2r_\rho^{-\varepsilon}\right)\right.\\
&\left.\times\int_0^{r_\rho^{-\varepsilon}} e^{-\rho r_\rho^2\int_{L_y} g(\|\boldsymbol{x}-\boldsymbol{y}\|)d\boldsymbol{x}} dy\right)
\end{aligned}
\tag{25}
$$

$$
\begin{aligned}
\leq&\lim_{\rho\to\infty}\rho^{\frac{1}{2}}r_\rho\int_0^{r_\rho^{-\varepsilon}} e^{-\rho r_\rho^2\int_{L_y} g(\|\boldsymbol{x}-\boldsymbol{y}\|)d\boldsymbol{x}} dy\\
=&\lim_{\rho\to\infty}\sqrt{\frac{\log\rho+b}{C}}\int_0^{r_\rho^{-\varepsilon}} e^{-\rho r_\rho^2\int_{L_y} g(\|\boldsymbol{x}-\boldsymbol{y}\|)d\boldsymbol{x}} dy\\
=&\lim_{\rho\to\infty}\sqrt{\frac{\log\rho+b}{C}}\left(\int_0^{\triangle} e^{-\rho r_\rho^2\int_{L_y} g(\|\boldsymbol{x}-\boldsymbol{y}\|)d\boldsymbol{x}} dy\right.\\
+&\left.\int_{\triangle}^{r_\rho^{-\varepsilon}} e^{-\rho r_\rho^2\int_{L_y} g(\|\boldsymbol{x}-\boldsymbol{y}\|)d\boldsymbol{x}} dy\right)
\end{aligned}
\tag{26}
$$

where in (25) $\boldsymbol{y}$ represents a (any) point in $\ell A_\rho$ at a Euclidean distance $y \in [0, r_\rho^{-\varepsilon}]$ apart from the border of $A_\rho$. Define $\lambda \triangleq \frac{\log \rho + b}{C}$ for convenience, it can be further shown that in (26)

$$
\begin{aligned}
& \lim_{\rho\to\infty} \sqrt{\lambda} \int_{\triangle}^{r_\rho^{-\varepsilon}} e^{-\rho r_\rho^2 \int_{L_y} g(\|\boldsymbol{x}-\boldsymbol{y}\|) d\boldsymbol{x}} dy \\
\leq\ & \lim_{\rho\to\infty} \sqrt{\lambda} \int_{\triangle}^{r_\rho^{-\varepsilon}} e^{-\rho r_\rho^2 \int_{C_y} g(\|\boldsymbol{x}-\boldsymbol{y}\|) d\boldsymbol{x}} dy \\
=\ & \lim_{\rho\to\infty} \sqrt{\lambda} \int_{\triangle}^{r_\rho^{-\varepsilon}} e^{-\frac{1}{2}\rho r_\rho^2 \int_0^y 2\pi x g(x) dx} dy \\
=\ & \lim_{\rho\to\infty} \sqrt{\lambda} \int_{\triangle}^{r_\rho^{-\varepsilon}} e^{-\frac{1}{2}\rho r_\rho^2 \left(\int_0^{\triangle} 2\pi x g(x) dx + \int_{\triangle}^y 2\pi x g(x) dx\right)} dy \\
\leq\ & \lim_{\rho\to\infty} \sqrt{\lambda} \int_{\triangle}^{r_\rho^{-\varepsilon}} e^{-\frac{1}{2}\rho r_\rho^2 \int_0^{\triangle} 2\pi x g(x) dx} dy \\
=\ & \lim_{\rho\to\infty} \sqrt{\lambda} \int_{\triangle}^{r_\rho^{-\varepsilon}} e^{-\gamma(\log\rho + b)} dy \qquad (27) \\
=\ & \lim_{\rho\to\infty} \sqrt{\lambda} \left( e^{-\gamma b} \rho^{-\gamma} \left( \left( \frac{\log\rho + b}{C\rho} \right)^{-\frac{\varepsilon}{2}} - \triangle \right) \right) \\
=\ & 0 \qquad (28)
\end{aligned}
$$

where (24) is used in reaching (27), and $\gamma > \frac{\varepsilon}{2}$ is used in reaching (28). It can also be shown that for the other term in (26),

$$
\begin{aligned}
& \lim_{\rho\to\infty} \sqrt{\frac{\log\rho + b}{C}} \int_0^{\triangle} e^{-\rho r_\rho^2 \int_{L_y} g(\|\boldsymbol{x}-\boldsymbol{y}\|) d\boldsymbol{x}} dy \\
\leq\ & \lim_{\rho\to\infty} \sqrt{\lambda} \int_0^{\triangle} e^{-\rho r_\rho^2 \int_{R_y} g(\|\boldsymbol{x}-\boldsymbol{y}\|) d\boldsymbol{x}} dy \qquad (29) \\
=\ & \lim_{\rho\to\infty} \sqrt{\lambda} \int_0^{\triangle} e^{-\rho r_\rho^2 2 \int_0^y \int_0^{\sqrt{r_\rho^{-2\varepsilon} - x^2}} g\left(\sqrt{x^2+z^2}\right) dz dx} dy \\
\leq\ & \lim_{\rho\to\infty} \sqrt{\lambda} \int_0^{\triangle} e^{-\rho r_\rho^2 2 \int_0^y \int_0^{r_\rho^{-\varepsilon} - x} g\left(\sqrt{x^2+z^2}\right) dz dx} dy \qquad (30) \\
\leq\ & \lim_{\rho\to\infty} \sqrt{\lambda} \int_0^{\triangle} e^{-\rho r_\rho^2 2 \int_0^y \int_0^{r_\rho^{-\varepsilon} - \triangle} g\left(\sqrt{x^2+z^2}\right) dz dx} dy \qquad (31) \\
\leq\ & \lim_{\rho\to\infty} \sqrt{\lambda} \int_0^{\triangle} e^{-\rho r_\rho^2 2 \int_0^y \int_0^{r_\rho^{-\varepsilon} - \triangle} g(z+\triangle) dz dx} dy \qquad (32) \\
=\ & \lim_{\rho\to\infty} \sqrt{\lambda} \int_0^{\triangle} e^{-\rho r_\rho^2 2y \int_0^{r_\rho^{-\varepsilon} - \triangle} g(z+\triangle) dz} dy \qquad (33)
\end{aligned}
$$

where (30) is obtained by noting that $r_\rho^{-2\varepsilon} - x^2 \geq \left(r_\rho^{-\varepsilon} - x\right)^2$ for $r_\rho^{-\varepsilon} \geq x$ (note that for $\rho$ sufficiently large, $r_\rho^{-\varepsilon} > \triangle \geq y \geq x$); (31) is obtained by noting that $x \leq \triangle$ and (32) is obtained by noting that $y \leq \triangle$ and the non-increasing property of $g$.

Let $\rho$ be sufficiently large such that $r_\rho^{-\varepsilon} \geq 2\triangle$ and also note that $g(\triangle) > 0$. Therefore $\beta \triangleq \int_0^{\triangle} g(z+\triangle) dz$ is a positive constant and $\beta > 0$. It then follows from (33) that

$$
\begin{aligned}
& \lim_{\rho\to\infty} \sqrt{\frac{\log\rho + b}{C}} \int_0^{\triangle} e^{-\rho r_\rho^2 \int_{L_y} g(\|\boldsymbol{x}-\boldsymbol{y}\|) d\boldsymbol{x}} dy \\
\leq\ & \lim_{\rho\to\infty} \sqrt{\frac{\log\rho + b}{C}} \int_0^{\triangle} e^{-\rho r_\rho^2 2\beta y} dy \\
=\ & \lim_{\rho\to\infty} \sqrt{\frac{\log\rho + b}{C}} \times \frac{1 - e^{-\rho r_\rho^2 2\beta\triangle}}{\rho r_\rho^2 2\beta} \\
=\ & \lim_{\rho\to\infty} \sqrt{\frac{\log\rho + b}{C}} \times \frac{1 - e^{-2\beta\triangle\frac{\log\rho+b}{C}}}{2\beta\frac{\log\rho+b}{C}} \\
=\ & 0 \qquad (34)
\end{aligned}
$$

As a result of (28) and (34), both terms on the right hand side of (26) go to zero and it follows that

$$\lim_{\rho\to\infty}\rho^{\frac{1}{2}}r_\rho^2\int_{\ell A_\rho}e^{-\rho r_\rho^2\int_{L_y}g(\|\boldsymbol{x}-\boldsymbol{y}\|)d\boldsymbol{x}}d\boldsymbol{y}=0$$

The above equation, together with (22) and (23), leads to the conclusion that

$$4\lim_{\rho\to\infty}\rho r_\rho^2\int_{\ell A_\rho}e^{-\rho r_\rho^2\int_{A_\rho}g(\|\boldsymbol{x}-\boldsymbol{y}\|)d\boldsymbol{x}}d\boldsymbol{y}=0 \tag{35}$$

i.e. the second term in (15) approaches $0$ as $\rho\to\infty$.

For the third term in (15), it can be shown that

$$\begin{aligned}
& 4\lim_{\rho\to\infty}\rho r_\rho^2\int_{\angle A_{\frac{1}{r_\rho}}}e^{-\rho r_\rho^2\int_{A_{\frac{1}{r_\rho}}}g(\|\boldsymbol{x}-\boldsymbol{y}\|)d\boldsymbol{x}}d\boldsymbol{y}\\
\le\ & 4\lim_{\rho\to\infty}\rho r_\rho^2\int_{\angle A_{\frac{1}{r_\rho}}}e^{-\rho r_\rho^2\int_{A_{\frac{1}{r_\rho}}\cap D\left(\boldsymbol{y},r_\rho^{-\varepsilon}\right)}g(\|\boldsymbol{x}-\boldsymbol{y}\|)d\boldsymbol{x}}d\boldsymbol{y}\\
\le\ & 4\lim_{\rho\to\infty}\rho r_\rho^2\int_{\angle A_{\frac{1}{r_\rho}}}e^{-\frac{1}{4}\rho r_\rho^2\int_{D\left(\boldsymbol{y},r_\rho^{-\varepsilon}\right)}g(\|\boldsymbol{x}-\boldsymbol{y}\|)d\boldsymbol{x}}d\boldsymbol{y}\\
=\ & 4\lim_{\rho\to\infty}\left(r_\rho^{-\varepsilon}\right)^2r_\rho^2\rho e^{-\frac{1}{4}\rho r_\rho^2\int_{D\left(\boldsymbol{y},r_\rho^{-\varepsilon}\right)}g(\|\boldsymbol{x}-\boldsymbol{y}\|)d\boldsymbol{x}}\\
=\ & 4\lim_{\rho\to\infty}r_\rho^{2-2\varepsilon}\rho e^{-\frac{1}{4}\rho r_\rho^2\left(C-\int_{\Re^2\setminus D\left(\boldsymbol{y},r_\rho^{-\varepsilon}\right)}g(\|\boldsymbol{x}-\boldsymbol{y}\|)d\boldsymbol{x}\right)}\\
=\ & 4\lim_{\rho\to\infty}\left(\frac{\log\rho+b}{C\rho}\right)^{1-\varepsilon}\rho e^{-\frac{1}{4}(\log\rho+b)} \qquad (36)\\
=\ & 4C^{-1+\varepsilon}e^{-\frac{1}{4}b}\lim_{\rho\to\infty}\frac{(\log\rho+b)^{1-\varepsilon}}{\rho^{\frac{1}{4}-\varepsilon}}\\
=\ & 0 \qquad (37)
\end{aligned}$$

where the second step results by noting that for any $\boldsymbol{y}\in\angle A_{\frac{1}{r_\rho}}$, $A_\rho\cap D\left(\boldsymbol{y},r_\rho^{-\varepsilon}\right)$ covers at least one quarter of $D\left(\boldsymbol{y},r_\rho^{-\varepsilon}\right)$, (19) is used in reaching (36), and $\varepsilon<\frac{1}{4}$ is used in the final step.

As a result of (15), (21), (35) and (37):

$$\lim_{\rho\to\infty}E(W)=e^{-b} \tag{38}$$

## Appendix II: Proof of Lemma 1

The torus that is commonly discussed in random geometric graph theory is essentially the same as a square except that the distance between two points on a torus is defined by their *toroidal distance*, instead of Euclidean distance. Thus a pair of nodes in $\mathcal{G}^T\left(\mathcal{X}_{\frac{\log\rho+b}{C}},g,A^T_{\frac{1}{r_\rho}}\right)$, located at $\boldsymbol{x}_1$ and $\boldsymbol{x}_2$ respectively, are directly connected with probability $g\left(\|\boldsymbol{x}_1-\boldsymbol{x}_2\|^T\right)$ where $\|\boldsymbol{x}_1-\boldsymbol{x}_2\|^T$ denotes the *toroidal distance* between the two nodes. For a unit torus $A^T=\left[-\frac{1}{2},\frac{1}{2}\right]^2$, the toroidal distance is given by [10, p. 13]:

$$\|\boldsymbol{x}_1-\boldsymbol{x}_2\|^T\triangleq\min\left\{\|\boldsymbol{x}_1+\boldsymbol{z}-\boldsymbol{x}_2\|:\boldsymbol{z}\in\mathbb{Z}^2\right\} \tag{39}$$

The toroidal distance between points on a torus of any other size can be computed analogously.

*Remark 5:* The use of toroidal distance allows nodes located near the boundary to have the same number of connections *probabilistically* as a node located near the center. Therefore it allows the removal of the boundary effect that is present in a square. The consideration of a torus implies that there is no need to consider special cases occurring near the boundary of the region and that events inside the region do not depend on the particular location inside the region. This often simplifies the analysis.

From now on, whenever the difference between a torus and a square affects the parameter being discussed, we use superscript $^T$ to mark the parameter in a torus.

We note the following relation between toroidal distance and Euclidean distance on a square area centered at the origin:

$$\|\boldsymbol{x}_1-\boldsymbol{x}_2\|^T\le\|\boldsymbol{x}_1-\boldsymbol{x}_2\| \tag{40}$$

$$\|\boldsymbol{x}\|^T=\|\boldsymbol{x}\| \tag{41}$$

which will be used in the later analysis.

It can then be shown that for an arbitrary node in $\mathcal{G}^T\left(\mathcal{X}_{\frac{\log\rho+b}{C}}, g, A^T_{\frac{1}{r_\rho}}\right)$ at location $\boldsymbol{y}$, the probability that it is isolated is given by:

$$\begin{aligned}\Pr\left(I^T_{\boldsymbol{y}}=1\right) &= e^{-\int_{A^T_{\frac{1}{r_\rho}}}\frac{\log\rho+b}{C}g\left(\|\boldsymbol{x}-\boldsymbol{y}\|^T\right)d\boldsymbol{x}}\\ &= e^{-\int_{A^T_{\frac{1}{r_\rho}}}\frac{\log\rho+b}{C}g\left(\|\boldsymbol{x}\|^T\right)d\boldsymbol{x}}\\ &= e^{-\int_{A_{\frac{1}{r_\rho}}}\frac{\log\rho+b}{C}g(\|\boldsymbol{x}\|)d\boldsymbol{x}}\end{aligned}$$

where in the second step, the property of a torus that the probability that an arbitrary node at location $\boldsymbol{y}$ is isolated is equal to the probability that a node at the origin is isolated is used; in the third step (41) is used.

Thus the expected number of isolated nodes in $\mathcal{G}^T\left(\mathcal{X}_{\frac{\log\rho+b}{C}}, g, A^T_{\frac{1}{r_\rho}}\right)$ is given by

$$\begin{aligned}& E\left(W^T\right)\\ =& \int_{A_{\frac{1}{r_\rho}}}\frac{\log\rho+b}{C}e^{-\int_{A_{\frac{1}{r_\rho}}}\frac{\log\rho+b}{C}g(\|\boldsymbol{x}\|)d\boldsymbol{x}}d\boldsymbol{y} \qquad (42)\\ =& \frac{1}{r_\rho^2}\frac{\log\rho+b}{C}e^{-\int_{A_{\frac{1}{r_\rho}}}\frac{\log\rho+b}{C}g(\|\boldsymbol{x}\|)d\boldsymbol{x}} \qquad (43)\\ =& \rho e^{-\int_{A_{\frac{1}{r_\rho}}}\frac{\log\rho+b}{C}g(\|\boldsymbol{x}\|)d\boldsymbol{x}} \qquad (44)\end{aligned}$$

First it can be shown using (6) that for $g$ satisfying (4)

$$\begin{aligned}& \lim_{\rho\to\infty}\rho e^{-\int_{D\left(\mathbf{0},r_\rho^{-\varepsilon}\right)}\frac{\log\rho+b}{C}g(\|\boldsymbol{x}\|)d\boldsymbol{x}}\\ =& \lim_{\rho\to\infty}\rho e^{-\frac{\log\rho+b}{C}\left(C-\int_{\Re^2\setminus D\left(\mathbf{0},r_\rho^{-\varepsilon}\right)}g(\|\boldsymbol{x}\|)d\boldsymbol{x}\right)}\\ =& e^{-b}\lim_{\rho\to\infty}e^{\frac{\log\rho+b}{C}\int_{r_\rho^{-\varepsilon}}^{\infty}2\pi x g(x)dx}\\ =& e^{-b} \qquad (45)\end{aligned}$$

where $D\left(\mathbf{0},x\right)$ denotes a disk centered at the origin and with a radius $x$, $\varepsilon$ is a small positive constant, and the last step results because

$$\begin{aligned}& \lim_{\rho\to\infty}\frac{\int_{r_\rho^{-\varepsilon}}^{\infty}2\pi x g\left(x\right)dx}{\frac{1}{\log\rho+b}}\\ =& \lim_{\rho\to\infty}\frac{\pi\varepsilon r_\rho^{-\varepsilon}g\left(r_\rho^{-\varepsilon}\right)r_\rho^{-\varepsilon-2}\frac{\log\rho+b-1}{C\rho^2}}{\frac{1}{\rho(\log\rho+b)^2}} \qquad (46)\\ =& \lim_{\rho\to\infty}\pi\varepsilon\left(\log\rho+b\right)^2 r_\rho^{-2\varepsilon}o_\rho\left(\frac{1}{r_\rho^{-2\varepsilon}\log^2\left(r_\rho^{-2\varepsilon}\right)}\right)\\ =& 0\end{aligned}$$

where L'Hôpital's rule is used in reaching (46) and in the third step $g\left(x\right)=o_x\left(\frac{1}{x^2\log^2 x}\right)$ is used. Note that by definition of $C$ in (6),

$$\rho e^{-\int_{\Re^2}\frac{\log\rho+b}{C}g(\|\boldsymbol{x}\|)d\boldsymbol{x}} = e^{-b} \qquad (47)$$

and

$$\begin{aligned}& \rho e^{-\int_{\Re^2}\frac{\log\rho+b}{C}g(\|\boldsymbol{x}\|)d\boldsymbol{x}}\\ \le& \rho e^{-\int_{A_{\frac{1}{r_\rho}}}\frac{\log\rho+b}{C}g(\|\boldsymbol{x}\|)d\boldsymbol{x}}\end{aligned}$$

$$\leq \quad \rho e^{-\int_{D\left(\mathbf{0}, r_\rho^{-\varepsilon}\right)} \frac{\log \rho + b}{C} g(\|\boldsymbol{x}\|) d\boldsymbol{x}} \tag{48}$$

As a result of (42), (45), (47) and (48)

$$\lim_{\rho\to\infty} E\left(W^T\right) \quad = \quad e^{-b} \tag{49}$$

## APPENDIX III PROOF OF THEOREM 4

In this Appendix, we give a proof of Theorem 4.

For convenience, let $\lambda$ be the node density in $\mathcal{G}\left(\mathcal{X}_{\frac{\log\rho+b}{C}}, g, A_{\frac{1}{r_\rho}}\right)$ where $\lambda \triangleq \rho r_\rho^2 = \frac{\log\rho+b}{C}$. Using the above notations, $\mathcal{G}\left(\mathcal{X}_{\frac{\log\rho+b}{C}}, g, A_{\frac{1}{r_\rho}}\right)$ can be written as $\mathcal{G}\left(\mathcal{X}_\lambda, g, A_{\frac{1}{r_\rho}}\right)$.

Note that for any finite $\rho$ the total number of nodes in $\mathcal{G}\left(\mathcal{X}_\lambda, g, A_{\frac{1}{r_\rho}}\right)$, hence the total number of components in $\mathcal{G}\left(\mathcal{X}_\lambda, g, A_{\frac{1}{r_\rho}}\right)$, is almost surely finite. Denote by $\xi_k$ the (random) number of components of order $k$ in an instance of $\mathcal{G}\left(\mathcal{X}_\lambda, g, A_{\frac{1}{r_\rho}}\right)$. It then suffices to show that for an arbitrarily large positive integer $M$:

$$\lim_{\rho\to\infty} \Pr\left(\sum_{k=2}^{M} \xi_k = 0\right) = 1 \tag{50}$$

The following symbols and notations are used in this appendix:

Denote by $g_1\left(\boldsymbol{x}_1, \boldsymbol{x}_2, \ldots, \boldsymbol{x}_k\right)$ the probability that a set of $k$ nodes at non-random positions $\boldsymbol{x}_1$, $\boldsymbol{x}_2$, …, $\boldsymbol{x}_k \in A_{\frac{1}{r_\rho}}$ forms a connected component.

Denote by $g_2\left(\boldsymbol{y}; \boldsymbol{x}_1, \boldsymbol{x}_2, \ldots, \boldsymbol{x}_k\right)$ the probability that a node at non-random position $\boldsymbol{y}$ is connected to at least one node in $\{\boldsymbol{x}_1, \boldsymbol{x}_2, \ldots, \boldsymbol{x}_k\}$. It can be shown that

$$g_2\left(\boldsymbol{y}; \boldsymbol{x}_1, \boldsymbol{x}_2, \ldots, \boldsymbol{x}_k\right) = 1 - \prod_{i=1}^{k} \left(1 - g\left(\|\boldsymbol{y} - \boldsymbol{x}_i\|\right)\right) \tag{51}$$

and

$$g_2\left(\boldsymbol{y}; \boldsymbol{x}_1, \boldsymbol{x}_2, \ldots, \boldsymbol{x}_k\right) \geq g_2\left(\boldsymbol{y}; \boldsymbol{x}_1, \boldsymbol{x}_2, \ldots, \boldsymbol{x}_i\right) \text{ for } 1 \leq i \leq k \tag{52}$$

As an easy consequence of the union bound,

$$g_2\left(\boldsymbol{y}; \boldsymbol{x}_1, \boldsymbol{x}_2, \ldots, \boldsymbol{x}_k\right) \leq \sum_{i=1}^{k} g\left(\|\boldsymbol{y} - \boldsymbol{x}_i\|\right) \tag{53}$$

Using the monotonicity and positive integral properties of $g$ in (1) and (2), it can be shown that there exists a positive constant $r$ such that $g\left(r^-\right)\left(1 - g\left(r^+\right)\right) > 0$ where $g\left(r^-\right) \triangleq \lim_{x\to r^-} g\left(x\right)$ and $g\left(r^+\right) \triangleq \lim_{x\to r^+} g\left(x\right)$. If $g$ is a continuous function, then $g\left(r^-\right) = g\left(r^+\right)$; if $g$ is a discontinuous function, e.g. a unit disk connection model, by choosing $r$ to be the transmission range, $g\left(r^-\right)\left(1 - g\left(r^+\right)\right) = 1$. For convenience in notations, we use $\beta$ for $g\left(r^-\right)\left(1 - g\left(r^+\right)\right)$, i.e.

$$\beta \triangleq g\left(r^-\right)\left(1 - g\left(r^+\right)\right) \tag{54}$$

Denote by $\partial A_{\frac{1}{r_\rho}}$ the border of $A_{\frac{1}{r_\rho}}$. Denote by $\ell A_{\frac{1}{r_\rho}} \subset A_{\frac{1}{r_\rho}}$ a rectangular area of size $\left(\frac{1}{r_\rho} - 2r\right) \times r$ along one side of the border of $A_{\frac{1}{r_\rho}}$, within a distance $r$ of the border and away from the four corners of $A_{\frac{1}{r_\rho}}$ by at least $r$. There are four such areas in $A_{\frac{1}{r_\rho}}$. Denote by $\angle A_{\frac{1}{r_\rho}} \subset A_{\frac{1}{r_\rho}}$ a square area of size $r \times r$ located at a corner of $A_{\frac{1}{r_\rho}}$. There are four such corner squares in $A_{\frac{1}{r_\rho}}$. Denote by $B_d\left(A_{\frac{1}{r_\rho}}\right) \subset A_{\frac{1}{r_\rho}}$ a boundary area within a distance $d$ of the border of $A_{\frac{1}{r_\rho}}$. Note the difference of the definitions of those symbols from those used Appendix I and particularly Fig. 2.

Let $D\left(\boldsymbol{x}, d\right) \subset \Re^2$ represents a disk centered at $\boldsymbol{x} \in A_{\frac{1}{r_\rho}}$ and with a radius $d$.

We first establish some preliminary results that will be used in the proof.

*Lemma 4:* In $\mathcal{G}\left(\mathcal{X}_\lambda, g, A_{\frac{1}{r_\rho}}\right)$, the expected number of components of order $k$ is given by

$$E\left(\xi_k\right) = \frac{\lambda^k}{k!} \int_{\left(A_{\frac{1}{r_\rho}}\right)^k} g_1\left(\boldsymbol{x}_1, \boldsymbol{x}_2, \ldots, \boldsymbol{x}_k\right) e^{-\lambda \int_{A_{\frac{1}{r_\rho}}} g_2\left(\boldsymbol{y}; \boldsymbol{x}_1, \boldsymbol{x}_2, \ldots, \boldsymbol{x}_k\right) d\boldsymbol{y}} d\left(\boldsymbol{x}_1 \cdots \boldsymbol{x}_k\right) \tag{55}$$

*Proof:* It can be shown that for any $n \geq k$:

$$E\left(\xi_k \left| |\mathcal{X}_\lambda| = n \right.\right) = \frac{\binom{n}{k}}{\left(A_{\frac{1}{r_\rho}}\right)^n} \int_{\left(A_{\frac{1}{r_\rho}}\right)^n} g_1\left(\boldsymbol{x}_1, \boldsymbol{x}_2, \ldots, \boldsymbol{x}_k\right) \prod_{i=k+1}^{n} \left(1 - g_2\left(\boldsymbol{x}_i; \boldsymbol{x}_1, \boldsymbol{x}_2, \ldots, \boldsymbol{x}_k\right)\right) d\left(\boldsymbol{x}_1 \cdots \boldsymbol{x}_n\right) \tag{56}$$

In (56), $\begin{pmatrix} n \\ k \end{pmatrix}$ is the number of distinct sets of $k$ nodes drawn from a total of $n$ nodes and the rest term represents the probability of the event that a *randomly chosen* set of $k$ nodes forms a component of order $k$. From (56), it follows that

$$\begin{aligned}
& E\left(\xi_k\right) \\
= & \sum_{n=k}^{\infty} E\left(\xi_k \left|\left|\mathcal{X}_\lambda\right| = n\right.\right) \frac{\left(\lambda A_{\frac{1}{r_\rho}}\right)^n}{n!} e^{-\lambda A_{\frac{1}{r_\rho}}} \\
= & \sum_{n=k}^{\infty} \frac{\left(\lambda A_{\frac{1}{r_\rho}}\right)^n}{n!} e^{-\lambda A_{\frac{1}{r_\rho}}} \frac{\begin{pmatrix} n \\ k \end{pmatrix}}{\left(A_{\frac{1}{r_\rho}}\right)^n} \int_{\left(A_{\frac{1}{r_\rho}}\right)^n} g_1\left(\boldsymbol{x}_1, \boldsymbol{x}_2, \ldots, \boldsymbol{x}_k\right) \prod_{i=k+1}^{n} \left(1 - g_2\left(\boldsymbol{x}_i; \boldsymbol{x}_1, \boldsymbol{x}_2, \ldots, \boldsymbol{x}_k\right)\right) d\left(\boldsymbol{x}_1 \cdots \boldsymbol{x}_n\right) \\
= & \sum_{n=k}^{\infty} \frac{\lambda^n}{n!} e^{-\lambda A_{\frac{1}{r_\rho}}} \begin{pmatrix} n \\ k \end{pmatrix} \int_{\left(A_{\frac{1}{r_\rho}}\right)^k} g_1\left(\boldsymbol{x}_1, \boldsymbol{x}_2, \ldots, \boldsymbol{x}_k\right) \left(\int_{A_{\frac{1}{r_\rho}}} 1 - g_2\left(\boldsymbol{y}; \boldsymbol{x}_1, \boldsymbol{x}_2, \ldots, \boldsymbol{x}_k\right) d\boldsymbol{y}\right)^{n-k} d\left(\boldsymbol{x}_1 \cdots \boldsymbol{x}_k\right) \\
= & \int_{\left(A_{\frac{1}{r_\rho}}\right)^k} g_1\left(\boldsymbol{x}_1, \boldsymbol{x}_2, \ldots, \boldsymbol{x}_k\right) \left(\sum_{n=k}^{\infty} \frac{\lambda^n}{n!} e^{-\lambda A_\rho} \begin{pmatrix} n \\ k \end{pmatrix} \left(\int_{A_{\frac{1}{r_\rho}}} 1 - g_2\left(\boldsymbol{y}; \boldsymbol{x}_1, \boldsymbol{x}_2, \ldots, \boldsymbol{x}_k\right) d\boldsymbol{y}\right)^{n-k}\right) d\left(\boldsymbol{x}_1 \cdots \boldsymbol{x}_k\right) \\
= & \frac{\lambda^k}{k!} \int_{\left(A_{\frac{1}{r_\rho}}\right)^k} g_1\left(\boldsymbol{x}_1, \boldsymbol{x}_2, \ldots, \boldsymbol{x}_k\right) \left(\sum_{n=k}^{\infty} \frac{\left(\lambda \left(\int_{A_{\frac{1}{r_\rho}}} 1 - g_2\left(\boldsymbol{y}; \boldsymbol{x}_1, \boldsymbol{x}_2, \ldots, \boldsymbol{x}_k\right) d\boldsymbol{y}\right)\right)^{n-k}}{(n-k)!} e^{-\lambda A_{\frac{1}{r_\rho}}}\right) d\left(\boldsymbol{x}_1 \cdots \boldsymbol{x}_k\right) \\
= & \frac{\lambda^k}{k!} \int_{\left(A_{\frac{1}{r_\rho}}\right)^k} g_1\left(\boldsymbol{x}_1, \boldsymbol{x}_2, \ldots, \boldsymbol{x}_k\right) e^{-\lambda \int_{A_{\frac{1}{r_\rho}}} g_2\left(\boldsymbol{y}; \boldsymbol{x}_1, \boldsymbol{x}_2, \ldots, \boldsymbol{x}_k\right) d\boldsymbol{y}} d\left(\boldsymbol{x}_1 \cdots \boldsymbol{x}_k\right)
\end{aligned}$$

■

A similar technique as that used in the proof of Proposition 6.2 in [2], originally due to Penrose [33], was used in the proof of Lemma 4 .

The following lemma is also used in the analysis of $E\left(\xi_k\right)$.

*Lemma 5:* A sufficient and necessary condition for a given set of nodes to form a single connected component is that there exists an ordering of the nodes, which can start from any node in the set, such that each node appearing later in the order is connected to at least one node appearing earlier in the order.

The proof is trivial and can be omitted.

Lemma 5 must have been proved in the literature as it forms the basis of a widely used algorithm to test network connectivity. However we are unable to find it.

Using Lemma 5, the following result can be established:

*Lemma 6:* Let $\Gamma_k$ denote the set $\{1, \ldots, k\}$. The function $g_1\left(\boldsymbol{x}_1, \boldsymbol{x}_2, \ldots, \boldsymbol{x}_k\right)$ satisfies the following inequality

$$\begin{aligned}
& g_1\left(\boldsymbol{x}_1, \boldsymbol{x}_2, \ldots, \boldsymbol{x}_k\right) \\
\leq & \sum_{i_2 \in \Gamma_k \backslash \{1\}, i_3 \in \Gamma_k \backslash \{1, i_2\}, \cdots, i_k \in \Gamma_k \backslash \{1, i_2, \ldots, i_{k-1}\}} g_2\left(\boldsymbol{x}_{i_2}; \boldsymbol{x}_1\right) g_2\left(\boldsymbol{x}_{i_3}; \boldsymbol{x}_1, \boldsymbol{x}_{i_2}\right) \cdots g_2\left(\boldsymbol{x}_{i_k}; \boldsymbol{x}_1, \boldsymbol{x}_{i_2}, \ldots, \boldsymbol{x}_{i_{k-1}}\right)
\end{aligned}$$

*Proof:* Without loss of generality, we assume that such ordering described in Lemma 5 starts from $\boldsymbol{x}_1 \in \{\boldsymbol{x}_1, \boldsymbol{x}_2, \ldots, \boldsymbol{x}_k\}$. Denote by $\xi_{(1, i_2, \ldots, i_k)}$ the event that $\left(\boldsymbol{x}_1, \boldsymbol{x}_{i_2}, \ldots, \boldsymbol{x}_{i_k}\right)$ is one of such an ordering described in Lemma 5, where $i_2 \in \Gamma_k \backslash \{1\}, i_3 \in \Gamma_k \backslash \{1, i_2\}, \cdots, i_k \in \Gamma_k \backslash \{1, i_2, \ldots, i_{k-1}\}$. Using Lemma 5, it can be shown that

$$\Pr\left(\xi_{(1, i_2, \ldots, i_{k-1})}\right) = g_2\left(\boldsymbol{x}_{i_2}; \boldsymbol{x}_1\right) g_2\left(\boldsymbol{x}_{i_3}; \boldsymbol{x}_1, \boldsymbol{x}_{i_2}\right) \cdots g_2\left(\boldsymbol{x}_{i_k}; \boldsymbol{x}_1, \boldsymbol{x}_{i_2}, \ldots, \boldsymbol{x}_{i_{k-1}}\right)$$

Then it follows that

$$g_1\left(\boldsymbol{x}_1, \boldsymbol{x}_2, \ldots, \boldsymbol{x}_k\right) = \Pr\left(\cup_{i_2 \in \Gamma_k \backslash \{1\}, i_3 \in \Gamma_k \backslash \{1, i_2\}, \cdots, i_k \in \Gamma_k \backslash \{1, i_2, \ldots, i_{k-1}\}} \xi_{(1, i_2, \ldots, i_k)}\right)$$

As an easy consequence of the above equation and the union bound:

$$g_1\left(\boldsymbol{x}_1, \boldsymbol{x}_2, \ldots, \boldsymbol{x}_k\right)$$

$$\leq \sum_{i_2\in\Gamma_k\backslash\{1\},i_3\in\Gamma_k\backslash\{1,i_2\},\cdots,i_k\in\Gamma_k\backslash\{1,i_2,\ldots,i_{k-1}\}} g_2\left(\boldsymbol{x}_{i_2};\boldsymbol{x}_1\right)g_2\left(\boldsymbol{x}_{i_3};\boldsymbol{x}_1,\boldsymbol{x}_{i_2}\right)\cdots g_2\left(\boldsymbol{x}_{i_k};\boldsymbol{x}_1,\boldsymbol{x}_{i_2},\ldots,\boldsymbol{x}_{i_{k-1}}\right)$$

■

The following geometric results are also used in the proof of Theorem 4.

*Lemma 7:* Consider two points $\boldsymbol{x}_1,\boldsymbol{x}_2\in A_{\frac{1}{r\rho}}$ and let $z\triangleq\|\boldsymbol{x}_2-\boldsymbol{x}_1\|$. For a positive constant $c_1=\sqrt{3}r$ and $z\leq r$

$$\left|D\left(\boldsymbol{x}_1,r\right)\backslash D\left(\boldsymbol{x}_2,r\right)\right|\geq c_1 z$$

where $\left|D\left(\boldsymbol{x}_1,r\right)\backslash D\left(\boldsymbol{x}_2,r\right)\right|$ denotes the area of $D\left(\boldsymbol{x}_1,r\right)\backslash D\left(\boldsymbol{x}_2,r\right)$.

*Proof:* First it can be shown that for $z\geq 2r$

$$\left|D\left(\boldsymbol{x}_1,r\right)\backslash D\left(\boldsymbol{x}_2,r\right)\right|=\pi r^2$$

and for $z<2r$

$$\begin{aligned}&f\left(z\right)\\ \triangleq\;&\left|D\left(\boldsymbol{x}_2,r\right)\backslash D\left(\boldsymbol{x}_1,r\right)\right|\\ =\;&\pi r^2-2r^2\arcsin\left(\sqrt{1-\frac{z^2}{4r^2}}\right)+zr\sqrt{1-\frac{z^2}{4r^2}}\end{aligned}$$

Further, it can be shown that

$$\frac{df\left(z\right)}{dz}=2r\sqrt{1-\frac{z^2}{4r^2}}$$

Therefore $f\left(z\right)$ is an increasing function of $z$ for $z<2r$ and $\frac{df(z)}{dz}\geq\sqrt{3}r$ for $z\leq r$. It then follows from $f\left(0\right)=0$ that $f\left(z\right)\geq\sqrt{3}rz$ for $z\leq r$. ■

*Lemma 8:* Consider two points $\boldsymbol{x}_1\in\ell A_{\frac{1}{r\rho}}$ and $\boldsymbol{x}_2\in A_{\frac{1}{r\rho}}\cap D\left(\boldsymbol{x}_1,r\right)$ and let $z\triangleq\|\boldsymbol{x}_2-\boldsymbol{x}_1\|$. When $\gamma\left(\boldsymbol{x}_2\right)\leq\gamma\left(\boldsymbol{x}_1\right)$,

$$\left|A_{\frac{1}{r\rho}}\cap D\left(\boldsymbol{x}_1,r\right)\backslash D\left(\boldsymbol{x}_2,r\right)\right|\geq\frac{c_1}{2}z$$

When $\gamma\left(\boldsymbol{x}_2\right)>\gamma\left(\boldsymbol{x}_1\right)$, for any positive constant $c_2$, there exists a positive constant $z_0<r$ such that for all $z\leq z_0$

$$\left|A_{\frac{1}{r\rho}}\cap D\left(\boldsymbol{x}_1,r\right)\backslash D\left(\boldsymbol{x}_2,r\right)\right|\geq\left(r-c_2\right)z-r\times\left|\gamma\left(\boldsymbol{x}_2\right)-\gamma\left(\boldsymbol{x}_1\right)\right|$$

where $\gamma\left(\boldsymbol{x}_1\right)$ ($\gamma\left(\boldsymbol{x}_2\right)$) represents the shortest Euclidean distance between $\boldsymbol{x}_1$ ($\boldsymbol{x}_2$) and a border of $A_{\frac{1}{r\rho}}$ that is adjacent to $\ell A_{\frac{1}{r\rho}}$ (i.e. $\partial A_{\frac{1}{r\rho}}\cap\ell A_{\frac{1}{r\rho}}$, see Fig. 4 for an illustration of $\gamma\left(\boldsymbol{x}_2\right)$ where $\gamma\left(\boldsymbol{x}_1\right)=0$ in the figure).

*Proof:* The first part of the lemma can be easily proved by noting that when $\gamma\left(\boldsymbol{x}_2\right)\leq\gamma\left(\boldsymbol{x}_1\right)$

$$\left|A_{\frac{1}{r\rho}}\cap D\left(\boldsymbol{x}_1,r\right)\backslash D\left(\boldsymbol{x}_2,r\right)\right|\geq\frac{1}{2}\left|D\left(\boldsymbol{x}_1,r\right)\backslash D\left(\boldsymbol{x}_2,r\right)\right|$$

and the lemma can then be proved using Lemma 7.

Now let us focus on the situation when $\gamma\left(\boldsymbol{x}_2\right)>\gamma\left(\boldsymbol{x}_1\right)$. It can be easily shown (see also Fig. 4) that when changing the value of $\gamma\left(\boldsymbol{x}_1\right)$ while keeping $\boldsymbol{x}_2-\boldsymbol{x}_1$ *fixed* (i.e. $\boldsymbol{x}_2$ has the same displacement as $\boldsymbol{x}_1$), $\left|A_{\frac{1}{r\rho}}\cap D\left(\boldsymbol{x}_1,r\right)\backslash D\left(\boldsymbol{x}_2,r\right)\right|$ is minimized as $\gamma\left(\boldsymbol{x}_1\right)=0$ (i.e. $\boldsymbol{x}_1\in\ell A_{\frac{1}{r\rho}}\cap\partial A_{\frac{1}{r\rho}}$) and $\left(r-c_2\right)z-r\times\left|\gamma\left(\boldsymbol{x}_2\right)-\gamma\left(\boldsymbol{x}_1\right)\right|$ remains constant. Therefore we focus on the worst case when $\boldsymbol{x}_1\in\ell A_{\frac{1}{r\rho}}\cap\partial A_{\frac{1}{r\rho}}$. When $\boldsymbol{x}_1\in\ell A_{\frac{1}{r\rho}}\cap\partial A_{\frac{1}{r\rho}}$, $\left|\gamma\left(\boldsymbol{x}_2\right)-\gamma\left(\boldsymbol{x}_1\right)\right|=\gamma\left(\boldsymbol{x}_2\right)$.

Fig. 4 shows $A_{\frac{1}{r\rho}}\cap D\left(\boldsymbol{x}_1,r\right)\backslash D\left(\boldsymbol{x}_2,r\right)$ for $\boldsymbol{x}_1\in\ell A_{\frac{1}{r\rho}}\cap\partial A_{\frac{1}{r\rho}}$ and $\boldsymbol{x}_2\in A_{\frac{1}{r\rho}}\cap D\left(\boldsymbol{x}_1,r\right)$. It can be shown that under the above conditions for $\boldsymbol{x}_1$ and $\boldsymbol{x}_2$ (see Fig. 4 for definitions of $\alpha$ and $A_1$ and some detailed but straightfoward geometric analysis omitted in the following equation)

$$\begin{aligned}&\left|A_\rho\cap D\left(\boldsymbol{x}_1,r\right)\backslash D\left(\boldsymbol{x}_2,r\right)\right|\\ \geq\;&\left|A_1\right|\\ =\;&h\left(z,\alpha\right)\\ \triangleq\;&\frac{\pi r^2}{4}-r^2\arccos\frac{z}{2r}+\frac{1}{2}zr\sqrt{1-\frac{z^2}{4r^2}}+\frac{r^2}{2}\arccos\frac{z\cos\alpha}{r}-\frac{1}{2}zr\sqrt{1-\frac{z^2}{r^2}\cos^2\alpha}\cos\alpha+\frac{1}{2}z^2\sin\alpha\cos\alpha\end{aligned}$$

Note that $h\left(0,\alpha\right)=0$,

$$\left.\frac{\partial h\left(z,\alpha\right)}{\partial z}\right|_{z=0}=r\left(1-\cos\alpha\right)$$

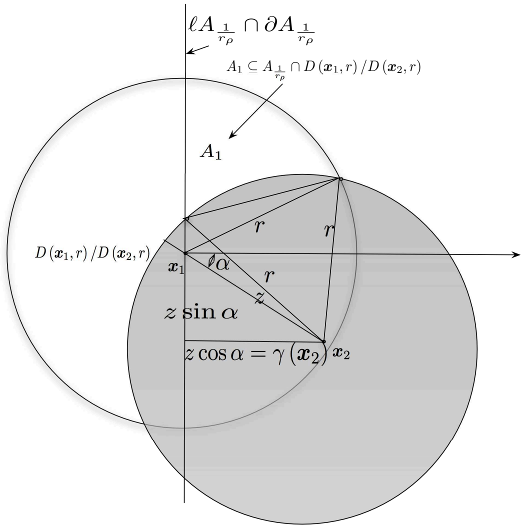


Figure 4: An illustration of $\left|A_{\frac{1}{r\rho}} \cap D(\boldsymbol{x}_2, r) / D(\boldsymbol{x}_1, r)\right|$ for $\boldsymbol{x}_1 \in \ell A_{\frac{1}{r\rho}} \cap \partial A_{\frac{1}{r\rho}}$ and $\boldsymbol{x}_2 \in A_{\frac{1}{r\rho}} \cap D(\boldsymbol{x}_1, r)$. Note that $A_1$ is the upper part of $A_\rho \cap D(\boldsymbol{x}_1, r) \backslash D(\boldsymbol{x}_2, r)$ above the line connecting $\boldsymbol{x}_1$ and $\boldsymbol{x}_2$. Depending on the relative positions of $\boldsymbol{x}_1$ and $\boldsymbol{x}_2$, $A_\rho \cap D(\boldsymbol{x}_1, r) \backslash D(\boldsymbol{x}_2, r)$ may also contain a non-empty region below the line connecting $\boldsymbol{x}_1$ and $\boldsymbol{x}_2$.

and $\cos\alpha = \frac{\gamma(\boldsymbol{x}_2)}{z}$. Therefore

$$\lim_{z \to 0^+} \frac{h(z, \alpha) - h(0, \alpha)}{z} = r(1 - \cos\alpha)$$

i.e. for a given positive constant $c_2$, there exists $z_\alpha > 0$ depending on $\alpha$ such that for all $0 \leq z \leq z_\alpha$

$$h(z, \alpha) \geq (r(1 - \cos\alpha) - c_2) z$$

The proof is complete by choosing $z_0 = \min_{0 \leq \alpha \leq \frac{\pi}{2}} z_\alpha$ and using $\cos\alpha = \frac{\gamma(\boldsymbol{x}_2)}{z}$.

■

On the basis of the above preliminary results, we are now ready to start the proof of Theorem 4.

Let $\delta$ be a positive constant and $\delta \leq \frac{r}{2}$. First, as a consequence of Lemma 4, it can be shown that

$$\begin{aligned}
& E(\xi_k) \\
= & \frac{\lambda^k}{k!} \int_{\left(A_{\frac{1}{r\rho}}\right)^{k-1}} \int_{A_{\frac{1}{r\rho}}} g_1(\boldsymbol{x}_1, \boldsymbol{x}_2, \ldots, \boldsymbol{x}_k) e^{-\lambda \int_{A_{\frac{1}{r\rho}}} g_2(\boldsymbol{y}; \boldsymbol{x}_1, \boldsymbol{x}_2, \ldots, \boldsymbol{x}_k) d\boldsymbol{y}} d\boldsymbol{x}_1 d(\boldsymbol{x}_2 \cdots \boldsymbol{x}_k) \\
= & \frac{\lambda^k}{k!} \int_{A_{\frac{1}{r\rho}}} \int_{\left(A_{\frac{1}{r\rho}}\right)^{k-1} \cap (D(\boldsymbol{x}_1, \delta))^{k-1}} g_1(\boldsymbol{x}_1, \boldsymbol{x}_2, \ldots, \boldsymbol{x}_k) e^{-\lambda \int_{A_{\frac{1}{r\rho}}} g_2(\boldsymbol{y}; \boldsymbol{x}_1, \boldsymbol{x}_2, \ldots, \boldsymbol{x}_k) d\boldsymbol{y}} d(\boldsymbol{x}_2 \cdots \boldsymbol{x}_k) d\boldsymbol{x}_1 \\
+ & \frac{\lambda^k}{k!} \int_{A_{\frac{1}{r\rho}}} \int_{\left(A_{\frac{1}{r\rho}}\right)^{k-1} \backslash (D(\boldsymbol{x}_1, \delta))^{k-1}} g_1(\boldsymbol{x}_1, \boldsymbol{x}_2, \ldots, \boldsymbol{x}_k) e^{-\lambda \int_{A_{\frac{1}{r\rho}}} g_2(\boldsymbol{y}; \boldsymbol{x}_1, \boldsymbol{x}_2, \ldots, \boldsymbol{x}_k) d\boldsymbol{y}} d(\boldsymbol{x}_2 \cdots \boldsymbol{x}_k) d\boldsymbol{x}_1
\end{aligned} \tag{57}$$

Denote by $E(\xi_{k,1})$ and $E(\xi_{k,2})$ the two summands in (57) respectively. In the following analysis, we will show that by choosing $\delta$ to be sufficiently small, $\lim_{\rho\to\infty} \sum_{k=2}^{\infty} E(\xi_{k.1}) = 0$ and $\lim_{\rho\to\infty} \sum_{k=2}^{M} E(\xi_{k,2}) = 0$. $\sum_{k=2}^{\infty} E(\xi_{k.1})$ has the meaning of being the expected total number of components of finite orders $\infty > k > 1$, where all other nodes of the component are located within a $\delta$ neighbourhood of a randomly designated node (i.e. $\boldsymbol{x}_1$ in (57)). $\lim_{\rho\to\infty} \sum_{k=2}^{\infty} E(\xi_{k.1}) = 0$ implies $\lim_{\rho\to\infty} \sum_{k=2}^{M} E(\xi_{k.1}) = 0$. $\sum_{k=2}^{M} E(\xi_{k,2}) = 0$ has the meaning of being the expected total number of components of finite orders $M \geq k > 1$ where at least one of the nodes forming the component is located outside a $\delta$ neighbourhood of a randomly designated node (i.e. $\boldsymbol{x}_1$ in (57)) in the component.

*An analysis of the first term in* (57)

Denote by $D_\delta^i \subset \left(A_{\frac{1}{r\rho}}\right)^{k-1}$ the set $\left\{(\boldsymbol{x}_2, \ldots, \boldsymbol{x}_k) \in \left(A_{\frac{1}{r\rho}}\right)^{k-1} \cap (D(\boldsymbol{x}_1, \delta))^{k-1} : \|\boldsymbol{x}_i - \boldsymbol{x}_1\| \geq \max_{j\in\{2,\ldots k\}, j\neq i} \|\boldsymbol{x}_j - \boldsymbol{x}_1\|\right\}$, $i \in \{2, \ldots k\}$. Using (52) and the definition of $D_\delta^i$, it can be shown that

$$
\begin{aligned}
& E\left(\xi_{k,1}\right) \\
\triangleq\; & \frac{\lambda^k}{k!}\int_{A_\rho}\int_{\left(A_{\frac{1}{r_\rho}}\right)^{k-1}\cap\left(D(\boldsymbol{x}_1,\delta)\right)^{k-1}} g_1\left(\boldsymbol{x}_1,\boldsymbol{x}_2,\ldots,\boldsymbol{x}_k\right)e^{-\lambda\int_{A_{\frac{1}{r_\rho}}} g_2(\boldsymbol{y};\boldsymbol{x}_1,\boldsymbol{x}_2,\ldots,\boldsymbol{x}_k)d\boldsymbol{y}}\, d\left(\boldsymbol{x}_2\cdots\boldsymbol{x}_k\right)d\boldsymbol{x}_1 \\
=\; & \sum_{i=2}^{k}\frac{\lambda^k}{k!}\int_{A_{\frac{1}{r_\rho}}}\int_{D_\delta^i} g_1\left(\boldsymbol{x}_1,\boldsymbol{x}_2,\ldots,\boldsymbol{x}_k\right)e^{-\lambda\int_{A_{\frac{1}{r_\rho}}} g_2(\boldsymbol{y};\boldsymbol{x}_1,\boldsymbol{x}_2,\ldots,\boldsymbol{x}_k)d\boldsymbol{y}}\, d\left(\boldsymbol{x}_2\cdots\boldsymbol{x}_k\right)d\boldsymbol{x}_1 \\
\le\; & \frac{\lambda^k}{(k-2)!k}\int_{A_{\frac{1}{r_\rho}}}\int_{D_\delta^2} g_1\left(\boldsymbol{x}_1,\boldsymbol{x}_2,\ldots,\boldsymbol{x}_k\right)e^{-\lambda\int_{A_{\frac{1}{r_\rho}}} g_2(\boldsymbol{y};\boldsymbol{x}_1,\boldsymbol{x}_2)d\boldsymbol{y}}\, d\left(\boldsymbol{x}_2\cdots\boldsymbol{x}_k\right)d\boldsymbol{x}_1 \\
\le\; & \frac{\lambda^k}{(k-2)!k}\int_{A_{\frac{1}{r_\rho}}}\int_{D_\delta^2} e^{-\lambda\int_{A_{\frac{1}{r_\rho}}} g_2(\boldsymbol{y};\boldsymbol{x}_1,\boldsymbol{x}_2)d\boldsymbol{y}}\, d\left(\boldsymbol{x}_2\cdots\boldsymbol{x}_k\right)d\boldsymbol{x}_1 \\
\le\; & \frac{\lambda^k}{(k-2)!k}\int_{A_{\frac{1}{r_\rho}}}\int_{A_{\frac{1}{r_\rho}}\cap D(\boldsymbol{x}_1,\delta)} \left(\pi\left\|\boldsymbol{x}_2-\boldsymbol{x}_1\right\|^2\right)^{k-2} e^{-\lambda\int_{A_{\frac{1}{r_\rho}}} g_2(\boldsymbol{y};\boldsymbol{x}_1,\boldsymbol{x}_2)d\boldsymbol{y}}\, d\boldsymbol{x}_2 d\boldsymbol{x}_1
\end{aligned}
\tag{58}
$$

As a result of the following inequality:

$$
\begin{aligned}
& \sum_{k=2}^{\infty}\frac{\lambda^k\left(\pi\left\|\boldsymbol{x}_2-\boldsymbol{x}_1\right\|^2\right)^{k-2}}{(k-2)!k} \\
=\; & \lambda^2\left(\sum_{k=0}^{\infty}\frac{\lambda^k\left(\pi\left\|\boldsymbol{x}_2-\boldsymbol{x}_1\right\|^2\right)^{k}}{k!\,(k+2)}\right) \\
\le\; & \lambda^2\left(\sum_{k=0}^{\infty}\frac{\lambda^k\left(\pi\left\|\boldsymbol{x}_2-\boldsymbol{x}_1\right\|^2\right)^{k}}{k!}e^{-\lambda\pi\left\|\boldsymbol{x}_2-\boldsymbol{x}_1\right\|^2}\right)e^{\lambda\pi\left\|\boldsymbol{x}_2-\boldsymbol{x}_1\right\|^2} \\
=\; & \lambda^2 e^{\lambda\pi\left\|\boldsymbol{x}_2-\boldsymbol{x}_1\right\|^2}
\end{aligned}
$$

it follows from (58) that

$$
\begin{aligned}
& \sum_{k=2}^{\infty}E\left(\xi_{k,1}\right) \\
\le\; & \lambda^2\int_{A_{\frac{1}{r_\rho}}}\int_{A_{\frac{1}{r_\rho}}\cap D(\boldsymbol{x}_1,\delta)} e^{-\lambda\left(\int_{A_{\frac{1}{r_\rho}}} g_2(\boldsymbol{y};\boldsymbol{x}_1,\boldsymbol{x}_2)d\boldsymbol{y}-\pi\|\boldsymbol{x}_2-\boldsymbol{x}_1\|^2\right)} d\boldsymbol{x}_2 d\boldsymbol{x}_1 \\
=\; & \lambda^2\int_{A_{\frac{1}{r_\rho}}}\int_{A_{\frac{1}{r_\rho}}\cap D(\boldsymbol{x}_1,\delta)} e^{-\lambda\left(\int_{A_{\frac{1}{r_\rho}}} g(\|\boldsymbol{y}-\boldsymbol{x}_2\|)d\boldsymbol{y}+\int_{A_{\frac{1}{r_\rho}}} g(\|\boldsymbol{y}-\boldsymbol{x}_1\|)(1-g(\|\boldsymbol{y}-\boldsymbol{x}_2\|))d\boldsymbol{y}-\pi\|\boldsymbol{x}_2-\boldsymbol{x}_1\|^2\right)} d\boldsymbol{x}_2 d\boldsymbol{x}_1 \\
\le\; & \lambda^2\int_{A_{\frac{1}{r_\rho}}}\int_{A_{\frac{1}{r_\rho}}\cap D(\boldsymbol{x}_1,\delta)} e^{-\lambda\left(\int_{A_{\frac{1}{r_\rho}}} g(\|\boldsymbol{y}-\boldsymbol{x}_2\|)d\boldsymbol{y}+\int_{A_{\frac{1}{r_\rho}}\cap D(\boldsymbol{x}_1,r)\setminus D(\boldsymbol{x}_2,r)} g(\|\boldsymbol{y}-\boldsymbol{x}_1\|)(1-g(\|\boldsymbol{y}-\boldsymbol{x}_2\|))d\boldsymbol{y}-\pi\|\boldsymbol{x}_2-\boldsymbol{x}_1\|^2\right)} d\boldsymbol{x}_2 d\boldsymbol{x}_1 && (59) \\
\le\; & \lambda^2\int_{A_{\frac{1}{r_\rho}}}\int_{A_{\frac{1}{r_\rho}}\cap D(\boldsymbol{x}_1,\delta)} e^{-\lambda\left(\int_{A_{\frac{1}{r_\rho}}} g(\|\boldsymbol{y}-\boldsymbol{x}_2\|)d\boldsymbol{y}+g\left(r^-\right)\left(1-g\left(r^+\right)\right)\left|A_{\frac{1}{r_\rho}}\cap D(\boldsymbol{x}_1,r)\setminus D(\boldsymbol{x}_2,r)\right|-\pi\|\boldsymbol{x}_2-\boldsymbol{x}_1\|^2\right)} d\boldsymbol{x}_2 d\boldsymbol{x}_1 && (60)
\end{aligned}
$$

where in (59) the parameter $r>0$ is chosen such that $g\left(r^-\right)\left(1-g\left(r^+\right)\right)>0$. For convenience, use $\beta$ for $g\left(r^-\right)\left(1-g\left(r^+\right)\right)$ as defined in (54). It follows from (60) that

$$
\sum_{k=2}^{\infty}E\left(\xi_{k,1}\right)
$$

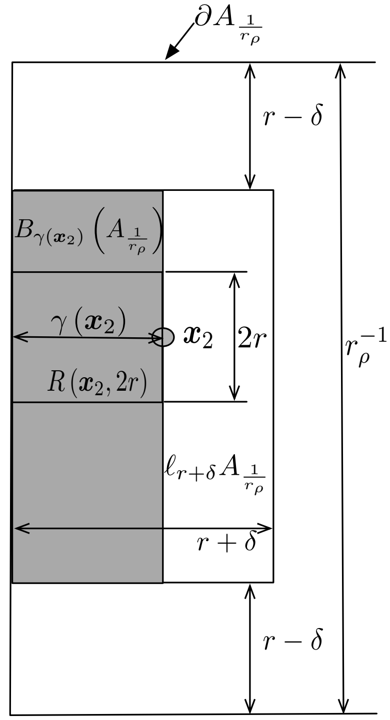


Figure 5: An illustration of the areas $\ell_{r+\delta}A_{\frac{1}{r_\rho}}$, $B_{\gamma(\boldsymbol{x}_2)}\left(A_{\frac{1}{r_\rho}}\right)$ and $R(\boldsymbol{x}_2, 2r)$. The shaded area is $B_{\gamma(\boldsymbol{x}_2)}\left(A_{\frac{1}{r_\rho}}\right)$.

$$\begin{aligned}
&\leq \lambda^2 \int_{B_r\left(A_{\frac{1}{r_\rho}}\right)} \int_{A_{\frac{1}{r_\rho}} \cap D(\boldsymbol{x}_1,\delta)} e^{-\lambda\left(\int_{A_{\frac{1}{r_\rho}}} g(\|\boldsymbol{y}-\boldsymbol{x}_2\|)d\boldsymbol{y} + \beta\left|A_{\frac{1}{r_\rho}} \cap D(\boldsymbol{x}_1,r)\backslash D(\boldsymbol{x}_2,r)\right| - \pi\|\boldsymbol{x}_2-\boldsymbol{x}_1\|^2\right)} d\boldsymbol{x}_2 d\boldsymbol{x}_1 \\
&+ \lambda^2 \int_{A_{\frac{1}{r_\rho}} \backslash B_r\left(A_{\frac{1}{r_\rho}}\right)} \int_{A_{\frac{1}{r_\rho}} \cap D(\boldsymbol{x}_1,\delta)} e^{-\lambda\left(\int_{A_{\frac{1}{r_\rho}}} g(\|\boldsymbol{y}-\boldsymbol{x}_2\|)d\boldsymbol{y} + \beta\left|A_{\frac{1}{r_\rho}} \cap D(\boldsymbol{x}_1,r)\backslash D(\boldsymbol{x}_2,r)\right| - \pi\|\boldsymbol{x}_2-\boldsymbol{x}_1\|^2\right)} d\boldsymbol{x}_2 d\boldsymbol{x}_1 \qquad (61)
\end{aligned}$$

For the first summand in the above equation, it can be shown that

$$\begin{aligned}
&\lambda^2 \int_{B_r\left(A_{\frac{1}{r_\rho}}\right)} \int_{A_{\frac{1}{r_\rho}} \cap D(\boldsymbol{x}_1,\delta)} e^{-\lambda\left(\int_{A_{\frac{1}{r_\rho}}} g(\|\boldsymbol{y}-\boldsymbol{x}_2\|)d\boldsymbol{y} + \beta\left|A_{\frac{1}{r_\rho}} \cap D(\boldsymbol{x}_1,r)\backslash D(\boldsymbol{x}_2,r)\right| - \pi\|\boldsymbol{x}_2-\boldsymbol{x}_1\|^2\right)} d\boldsymbol{x}_2 d\boldsymbol{x}_1 \\
&= 4\lambda^2 \int_{\ell A_{\frac{1}{r_\rho}}} \int_{A_{\frac{1}{r_\rho}} \cap D(\boldsymbol{x}_1,\delta)} e^{-\lambda\left(\int_{A_{\frac{1}{r_\rho}}} g(\|\boldsymbol{y}-\boldsymbol{x}_2\|)d\boldsymbol{y} + \beta\left|A_{\frac{1}{r_\rho}} \cap D(\boldsymbol{x}_1,r)\backslash D(\boldsymbol{x}_2,r)\right| - \pi\|\boldsymbol{x}_2-\boldsymbol{x}_1\|^2\right)} d\boldsymbol{x}_2 d\boldsymbol{x}_1 \\
&+ 4\lambda^2 \int_{\angle A_{\frac{1}{r_\rho}}} \int_{A_{\frac{1}{r_\rho}} \cap D(\boldsymbol{x}_1,\delta)} e^{-\lambda\left(\int_{A_{\frac{1}{r_\rho}}} g(\|\boldsymbol{y}-\boldsymbol{x}_2\|)d\boldsymbol{y} + \beta\left|A_{\frac{1}{r_\rho}} \cap D(\boldsymbol{x}_1,r)\backslash D(\boldsymbol{x}_2,r)\right| - \pi\|\boldsymbol{x}_2-\boldsymbol{x}_1\|^2\right)} d\boldsymbol{x}_2 d\boldsymbol{x}_1 \qquad (62)
\end{aligned}$$

Denote by $\gamma(\boldsymbol{x})$ the shortest Euclidean distance between a point $\boldsymbol{x} \in \ell_{r+\delta}A_{\frac{1}{r_\rho}}$ and a border of $A_{\frac{1}{r_\rho}}$ adjacent to $\ell_{r+\delta}A_{\frac{1}{r_\rho}}$ (i.e. $\partial A_{\frac{1}{r_\rho}} \cap \ell_{r+\delta}A_{\frac{1}{r_\rho}}$), where $\ell_{r+\delta}A_{\frac{1}{r_\rho}}$ denotes a boundary rectangular area of size $\left(r_\rho^{-1} - 2(r-\delta)\right) \times (r+\delta)$ within $r+\delta$ of the border of $A_{\frac{1}{r_\rho}}$ and away from the corners of $A_{\frac{1}{r_\rho}}$ by at least $r-\delta$. Denote by $B_{\gamma(\boldsymbol{x}_2)}\left(A_{\frac{1}{r_\rho}}\right) \subset A_\rho$ a boundary area $\left\{\boldsymbol{x} \in \ell_{r+\delta}A_{\frac{1}{r_\rho}} : \gamma(\boldsymbol{x}) \leq \gamma(\boldsymbol{x}_2)\right\}$, denote by $R(\boldsymbol{x}_2, 2r)$ a rectangular area of size $2r \times \gamma(\boldsymbol{x}_2)$ located between $\boldsymbol{x}_2$ and $\partial A_{\frac{1}{r_\rho}}$ with $\boldsymbol{x}_2$ at the center of one side of $R(\boldsymbol{x}_2, 2r)$. See Fig. 5 for an illustration of the areas defined above.

First we evaluate the term: $\int_{B_{\gamma(\boldsymbol{x}_2)}\left(A_{\frac{1}{r_\rho}}\right)} g(\|\boldsymbol{y}-\boldsymbol{x}_2\|)\, d\boldsymbol{y} + \beta\left|A_{\frac{1}{r_\rho}} \cap D(\boldsymbol{x}_1, r) \backslash D(\boldsymbol{x}_2, r)\right|$. It can be shown that for $\boldsymbol{x}_1 \in$

$\ell A_{\frac{1}{r\rho}}$ and $\boldsymbol{x}_2 \in A_{\frac{1}{r\rho}} \cap D(\boldsymbol{x}_1, \delta)$, when $\gamma(\boldsymbol{x}_2) \geq \gamma(\boldsymbol{x}_1)$:

$$\begin{aligned}
& \int_{B_{\gamma(\boldsymbol{x}_2)}\left(A_{\frac{1}{r\rho}}\right)} g(\|\boldsymbol{y}-\boldsymbol{x}_2\|)\, d\boldsymbol{y} \\
\geq\; & \int_{B_{\gamma(\boldsymbol{x}_2)}\left(A_{\frac{1}{r\rho}}\right)\cap R(\boldsymbol{x}_2, 2r)} g(\|\boldsymbol{y}-\boldsymbol{x}_2\|)\, d\boldsymbol{y} \\
\geq\; & \int_0^r \int_0^{\gamma(\boldsymbol{x}_2)} g\left(\sqrt{x^2+y^2}\right) dx dy \\
\geq\; & \int_0^r \int_0^{|\gamma(\boldsymbol{x}_2)-\gamma(\boldsymbol{x}_1)|} g\left(\sqrt{x^2+y^2}\right) dx dy \\
\geq\; & \int_0^r \int_0^{|\gamma(\boldsymbol{x}_2)-\gamma(\boldsymbol{x}_1)|} g\left(\sqrt{\left(\frac{r}{2}\right)^2+y^2}\right) dx dy \qquad (63) \\
=\; & c_3 \left|\gamma(\boldsymbol{x}_2)-\gamma(\boldsymbol{x}_1)\right|
\end{aligned}$$

where in (63), the non-increasing monotonicity condition on $g$ and that $|\gamma(\boldsymbol{x}_2)-\gamma(\boldsymbol{x}_1)| \leq \|\boldsymbol{x}_2-\boldsymbol{x}_1\| \leq \delta \leq \frac{r}{2}$ is used, and $c_3 \triangleq \int_0^r g\left(\sqrt{\left(\frac{r}{2}\right)^2+y^2}\right) dy$. Since $g(r^-)(1-g(r^+)) > 0$, it follows from the non-increasing monotonicity condition on $g$ that $g\left(\frac{r}{2}\right) > 0$ and $c_3$ is a positive constant, i.e. $c_3 > 0$.

Choose $c_2$ to be sufficiently small such that $c_4 \triangleq \frac{c_3}{\beta} - c_2 > 0$ and choose $\delta$ to be sufficiently small such that $\delta \leq z_0$. Using (63) and Lemma 8, it follows that

$$\begin{aligned}
& \int_{B_{\gamma(\boldsymbol{x}_2)}\left(A_{\frac{1}{r\rho}}\right)} g(\|\boldsymbol{y}-\boldsymbol{x}_2\|)\, d\boldsymbol{y} + \beta \left|A_{\frac{1}{r\rho}} \cap D(\boldsymbol{x}_1, r) \setminus D(\boldsymbol{x}_2, r)\right| \\
\geq\; & c_3 |\gamma(\boldsymbol{x}_2)-\gamma(\boldsymbol{x}_1)| + \beta\left((r-c_2)\|\boldsymbol{x}_2-\boldsymbol{x}_1\| - r \times |\gamma(\boldsymbol{x}_2)-\gamma(\boldsymbol{x}_1)|\right) \\
=\; & \beta\left((r-c_2) - \left(r - \frac{c_3}{\beta}\right) \times \frac{|\gamma(\boldsymbol{x}_2)-\gamma(\boldsymbol{x}_1)|}{\|\boldsymbol{x}_2-\boldsymbol{x}_1\|}\right) \|\boldsymbol{x}_2-\boldsymbol{x}_1\|
\end{aligned}$$

Note that $\frac{|\gamma(\boldsymbol{x}_2)-\gamma(\boldsymbol{x}_1)|}{\|\boldsymbol{x}_2-\boldsymbol{x}_1\|} \leq 1$, therefore

$$(r-c_2) - \left(r - \frac{c_3}{\beta}\right) \times \frac{|\gamma(\boldsymbol{x}_2)-\gamma(\boldsymbol{x}_1)|}{\|\boldsymbol{x}_2-\boldsymbol{x}_1\|} \geq \frac{c_3}{\beta} - c_2$$

$$\begin{aligned}
& \int_{B_{\gamma(\boldsymbol{x}_2)}\left(A_{\frac{1}{r\rho}}\right)} g(\|\boldsymbol{y}-\boldsymbol{x}_2\|)\, d\boldsymbol{y} + \beta \left|A_{\frac{1}{r\rho}} \cap D(\boldsymbol{x}_1, r) \setminus D(\boldsymbol{x}_2, r)\right| \\
\geq\; & \beta c_4 \|\boldsymbol{x}_2-\boldsymbol{x}_1\| \qquad (64)
\end{aligned}$$

When $\gamma(\boldsymbol{x}_2) < \gamma(\boldsymbol{x}_1)$, using Lemma 8

$$\begin{aligned}
& \int_{B_{\gamma(\boldsymbol{x}_2)}\left(A_{\frac{1}{r\rho}}\right)} g(\|\boldsymbol{y}-\boldsymbol{x}_2\|)\, d\boldsymbol{y} + \beta \left|A_{\frac{1}{r\rho}} \cap D(\boldsymbol{x}_1, r) \setminus D(\boldsymbol{x}_2, r)\right| \\
\geq\; & \beta \left|A_{\frac{1}{r\rho}} \cap D(\boldsymbol{x}_1, r) \setminus D(\boldsymbol{x}_2, r)\right| \\
\geq\; & \beta \frac{c_1}{2} \|\boldsymbol{x}_2-\boldsymbol{x}_1\| \qquad (65)
\end{aligned}$$

Let $c_5 \triangleq \min\left\{\frac{c_1}{2}, c_4\right\}$. It follows from (64) and (65) that

$$\begin{aligned}
& \int_{B_{\gamma(\boldsymbol{x}_2)}\left(A_{\frac{1}{r\rho}}\right)} g(\|\boldsymbol{y}-\boldsymbol{x}_2\|)\, d\boldsymbol{y} + \beta \left|A_{\frac{1}{r\rho}} \cap D(\boldsymbol{x}_1, r) \setminus D(\boldsymbol{x}_2, r)\right| \\
\geq\; & \beta c_5 \|\boldsymbol{x}_2-\boldsymbol{x}_1\|
\end{aligned}$$

Choose $\delta$ to be sufficiently small such that $\pi\delta \leq \frac{1}{2}c_5\beta$ and also $\delta \leq z_0$. Note also that for $\boldsymbol{x}_2 \in A_{\frac{1}{r\rho}} \cap D(\boldsymbol{x}_1, \delta)$, $\|\boldsymbol{x}_2-\boldsymbol{x}_1\| \leq \delta$. Then it follows that

$$4\lambda^2 \int_{\ell A_{\frac{1}{r\rho}}} \int_{A_{\frac{1}{r\rho}} \cap D(\boldsymbol{x}_1, \delta)} e^{-\lambda\left(\int_{A_{\frac{1}{r\rho}}} g(\|\boldsymbol{y}-\boldsymbol{x}_2\|)d\boldsymbol{y} + \beta\left|A_{\frac{1}{r\rho}} \cap D(\boldsymbol{x}_1, r)\setminus D(\boldsymbol{x}_2, r)\right| - \pi\|\boldsymbol{x}_2-\boldsymbol{x}_1\|^2\right)} d\boldsymbol{x}_2 d\boldsymbol{x}_1$$

$$\begin{aligned}
&\leq 4\lambda^2 \int_{\ell A_{\frac{1}{r_\rho}}} \int_{A_{\frac{1}{r_\rho}} \cap D(\boldsymbol{x}_1,\delta)} e^{-\lambda\left(\int_{A_{\frac{1}{r_\rho}} \setminus B_{\gamma(\boldsymbol{x}_2)}\left(A_{\frac{1}{r_\rho}}\right)} g(\|\boldsymbol{y}-\boldsymbol{x}_2\|)d\boldsymbol{y} + \frac{1}{2}c_5\beta\|\boldsymbol{x}_2-\boldsymbol{x}_1\|\right)} d\boldsymbol{x}_2 d\boldsymbol{x}_1 \\
&\leq 4\lambda^2 \int_{\ell_{r+\delta} A_{\frac{1}{r_\rho}}} \int_{A_{\frac{1}{r_\rho}} \cap D(\boldsymbol{x}_2,\delta)} e^{-\lambda\left(\int_{A_{\frac{1}{r_\rho}} \setminus B_{\gamma(\boldsymbol{x}_2)}\left(A_{\frac{1}{r_\rho}}\right)} g(\|\boldsymbol{y}-\boldsymbol{x}_2\|)d\boldsymbol{y} + \frac{1}{2}c_5\beta\|\boldsymbol{x}_2-\boldsymbol{x}_1\|\right)} d\boldsymbol{x}_1 d\boldsymbol{x}_2 \\
&\leq 4\lambda^2 \int_0^\delta e^{-\lambda\frac{1}{2}c_5\beta x} 2\pi x dx \int_{\ell_{r+\delta} A_{\frac{1}{r_\rho}}} e^{-\lambda\int_{A_{\frac{1}{r_\rho}} \setminus B_{\gamma(\boldsymbol{x}_2)}\left(A_{\frac{1}{r_\rho}}\right)} g(\|\boldsymbol{y}-\boldsymbol{x}_2\|)d\boldsymbol{y}} d\boldsymbol{x}_2 \\
&= 32\pi \frac{1-e^{-\lambda\frac{1}{2}c_5\beta\delta}\left(1+\lambda\frac{1}{2}c_5\beta\delta\right)}{(c_5\beta)^2} \int_{\ell_{r+\delta} A_{\frac{1}{r_\rho}}} e^{-\lambda\int_{A_{\frac{1}{r_\rho}} \setminus B_{\gamma(\boldsymbol{x}_2)}\left(A_{\frac{1}{r_\rho}}\right)} g(\|\boldsymbol{y}-\boldsymbol{x}_2\|)d\boldsymbol{y}} d\boldsymbol{x}_2
\end{aligned}$$

We further divide $\ell_{r+\delta} A_{\frac{1}{r_\rho}}$ into two parts: one rectangular area of size $\left(r_\rho^{-1} - 2r_\rho^{-\varepsilon}\right) \times (r+\delta)$ in the center of $\ell_{r+\delta} A_{\frac{1}{r_\rho}}$, denoted by $\ell^1_{r+\delta} A_{\frac{1}{r_\rho}}$, and the other area $\ell^2_{r+\delta} A_\rho = \ell_{r+\delta} A_{\frac{1}{r_\rho}} \backslash \ell^1_{r+\delta} A_{\frac{1}{r_\rho}}$ . It can be shown that

$$\begin{aligned}
&\lim_{\rho\to\infty} \int_{\ell^1_{r+\delta} A_{\frac{1}{r_\rho}}} e^{-\lambda\int_{A_{\frac{1}{r_\rho}} \setminus B_{\gamma(\boldsymbol{x}_2)}\left(A_{\frac{1}{r_\rho}}\right)} g(\|\boldsymbol{y}-\boldsymbol{x}_2\|)d\boldsymbol{y}} d\boldsymbol{x}_2 \\
\leq\ &\lim_{\rho\to\infty} \int_{\ell^1_{r+\delta} A_{\frac{1}{r_\rho}}} e^{-\lambda\int_{A_{\frac{1}{r_\rho}} \setminus B_{\gamma(\boldsymbol{x}_2)}\left(A_{\frac{1}{r_\rho}}\right) \cap D\left(\boldsymbol{x}_2, r_\rho^{-\varepsilon}\right)} g(\|\boldsymbol{y}-\boldsymbol{x}_2\|)d\boldsymbol{y}} d\boldsymbol{x}_2 \\
=\ &\lim_{\rho\to\infty} \left(r_\rho^{-1} - 2r_\rho^{-\varepsilon}\right) \times (r+\delta)\, e^{-\frac{1}{2}\lambda\int_{D\left(\boldsymbol{0}, r_\rho^{-\varepsilon}\right)} g(\|\boldsymbol{y}\|)d\boldsymbol{y}} \\
=\ &0
\end{aligned} \tag{66}$$

where the last step results due to (23), which showed that for $g$ satisfying both (1) and (4) $\lim_{\rho\to\infty} \rho^{\frac{1}{2}} e^{-\frac{1}{2}\rho r_\rho^2 \int_{D\left(\boldsymbol{0}, r_\rho^{-\varepsilon}\right)} g(\|\boldsymbol{x}\|)d\boldsymbol{x}} = e^{-\frac{b}{2}}$. Then the result follows easily from the definition of $r_\rho$ in (5). Note that the result in (66) cannot be obtained for $g$ satisfying (1) and (2) only.

Using similar steps that resulted in (37), it can be shown that

$$\lim_{\rho\to\infty} \int_{\ell^2_{r+\delta} A_{\frac{1}{r_\rho}}} e^{-\lambda\int_{A_{\frac{1}{r_\rho}} \setminus B_{\gamma(\boldsymbol{x}_2)}\left(A_{\frac{1}{r_\rho}}\right)} g(\|\boldsymbol{y}-\boldsymbol{x}_2\|)d\boldsymbol{y}} d\boldsymbol{x}_2 = 0$$

The above equation, together with (66), allows us to conclude that the first term in (62) converges to $0$ as $\rho \to \infty$:

$$\lim_{\rho\to\infty} 4\lambda^2 \int_{\ell A_{\frac{1}{r_\rho}}} \int_{A_{\frac{1}{r_\rho}} \cap D(\boldsymbol{x}_1,\delta)} e^{-\lambda\left(\int_{A_{\frac{1}{r_\rho}}} g(\|\boldsymbol{y}-\boldsymbol{x}_2\|)d\boldsymbol{y} + \beta\left|A_{\frac{1}{r_\rho}} \cap D(\boldsymbol{x}_1,r) \backslash D(\boldsymbol{x}_2,r)\right| - \pi\|\boldsymbol{x}_2-\boldsymbol{x}_1\|^2\right)} d\boldsymbol{x}_2 d\boldsymbol{x}_1 = 0 \tag{67}$$

Now let us consider the second term in (62). First it can be shown that

$$\int_{A_{\frac{1}{r_\rho}}} g\left(\|\boldsymbol{y}-\boldsymbol{x}_2\|\right) d\boldsymbol{y} \geq \int_{A_{\frac{1}{r_\rho}} \cap D\left(\boldsymbol{x}_2, r_\rho^{-\varepsilon}\right)} g\left(\|\boldsymbol{y}-\boldsymbol{x}_2\|\right) d\boldsymbol{y}$$

and for any $\boldsymbol{x}_2 \in A_{\frac{1}{r_\rho}}$, $A_{\frac{1}{r_\rho}} \cap D\left(\boldsymbol{x}_2, r_\rho^{-\varepsilon}\right)$ contains at least one quarter of $D\left(\boldsymbol{x}_2, r_\rho^{-\varepsilon}\right)$. Further, since

$$\lim_{\rho\to\infty} \int_{D\left(\boldsymbol{x}_2, r_\rho^{-\varepsilon}\right)} g\left(\|\boldsymbol{y}-\boldsymbol{x}_2\|\right) d\boldsymbol{y} = C$$

there exists a $\rho_0$ such that for $\rho \geq \rho_0$ and any positive constant $\gamma < 1$

$$\int_{D\left(\boldsymbol{x}_2, r_\rho^{-\varepsilon}\right)} g\left(\|\boldsymbol{y}-\boldsymbol{x}_2\|\right) d\boldsymbol{y} \geq \gamma C$$

As a result of the above discussions, it can be shown that for sufficiently large $\rho \geq \rho_0$

$$\begin{aligned} & 4\lambda^2 \int_{\angle A_{\frac{1}{r_\rho}}} \int_{A_{\frac{1}{r_\rho}} \cap D(\boldsymbol{x}_1,\delta)} e^{-\lambda\left(\int_{A_{\frac{1}{r_\rho}}} g(\|\boldsymbol{y}-\boldsymbol{x}_2\|)d\boldsymbol{y}+\beta\left|A_{\frac{1}{r_\rho}}\cap D(\boldsymbol{x}_1,r)\backslash D(\boldsymbol{x}_2,r)\right|-\pi\|\boldsymbol{x}_2-\boldsymbol{x}_1\|^2\right)} d\boldsymbol{x}_2 d\boldsymbol{x}_1 \\ \leq \; & 4\lambda^2 \int_{\angle A_{\frac{1}{r_\rho}}} \int_{A_{\frac{1}{r_\rho}} \cap D(\boldsymbol{x}_1,\delta)} e^{-\lambda\left(\frac{1}{4}\gamma C-\pi\|\boldsymbol{x}_2-\boldsymbol{x}_1\|^2\right)} d\boldsymbol{x}_2 d\boldsymbol{x}_1 \\ \leq \; & 4\lambda^2\pi\delta^2 r^2 e^{-\lambda\left(\frac{1}{4}\gamma C-\pi\delta^2\right)} \end{aligned} \tag{68}$$

where by choosing $\delta < \frac{1}{4\pi}\gamma C$, the above equation can be easily shown as converging to $0$ as $\rho \to \infty$.

In summary, using (62), (67) and (68), it can be shown that for $\delta < \min\left\{\frac{1}{4\pi}\gamma C, \frac{r}{2}, \frac{1}{2\pi}c_5\beta, z_0\right\}$, for the first term in (61), we have

$$\lim_{\rho\to\infty} \lambda^2 \int_{B_r\left(A_{\frac{1}{r_\rho}}\right)} \int_{A_{\frac{1}{r_\rho}} \cap D(\boldsymbol{x}_1,\delta)} e^{-\lambda\left(\int_{A_{\frac{1}{r_\rho}}} g(\|\boldsymbol{y}-\boldsymbol{x}_2\|)d\boldsymbol{y}+\beta\left|A_{\frac{1}{r_\rho}}\cap D(\boldsymbol{x}_1,r)\backslash D(\boldsymbol{x}_2,r)\right|-\pi\|\boldsymbol{x}_2-\boldsymbol{x}_1\|^2\right)} d\boldsymbol{x}_2 d\boldsymbol{x}_1 = 0 \tag{69}$$

For the second term in (61), using Lemma 7, it can be shown that

$$\begin{aligned} & \lambda^2 \int_{A_{\frac{1}{r_\rho}} \backslash B_r\left(A_{\frac{1}{r_\rho}}\right)} \int_{A_{\frac{1}{r_\rho}} \cap D(\boldsymbol{x}_1,\delta)} e^{-\lambda\left(\int_{A_{\frac{1}{r_\rho}}} g(\|\boldsymbol{y}-\boldsymbol{x}_2\|)d\boldsymbol{y}+\beta\left|A_{\frac{1}{r_\rho}}\cap D(\boldsymbol{x}_1,r)\backslash D(\boldsymbol{x}_2,r)\right|-\pi\|\boldsymbol{x}_2-\boldsymbol{x}_1\|^2\right)} d\boldsymbol{x}_2 d\boldsymbol{x}_1 \\ = \; & \lambda^2 \int_{A_{\frac{1}{r_\rho}} \backslash B_r\left(A_{\frac{1}{r_\rho}}\right)} \int_{A_{\frac{1}{r_\rho}} \cap D(\boldsymbol{x}_1,\delta)} e^{-\lambda\left(\int_{A_{\frac{1}{r_\rho}}} g(\|\boldsymbol{y}-\boldsymbol{x}_2\|)d\boldsymbol{y}+\beta|D(\boldsymbol{x}_1,r)\backslash D(\boldsymbol{x}_2,r)|-\pi\|\boldsymbol{x}_2-\boldsymbol{x}_1\|^2\right)} d\boldsymbol{x}_2 d\boldsymbol{x}_1 \\ \leq \; & \lambda^2 \int_{A_{\frac{1}{r_\rho}} \backslash B_r\left(A_{\frac{1}{r_\rho}}\right)} \int_{A_{\frac{1}{r_\rho}} \cap D(\boldsymbol{x}_1,\delta)} e^{-\lambda\left(\int_{A_{\frac{1}{r_\rho}}} g(\|\boldsymbol{y}-\boldsymbol{x}_2\|)d\boldsymbol{y}+\left(\beta\sqrt{3}r-\pi\delta\right)\|\boldsymbol{x}_2-\boldsymbol{x}_1\|\right)} d\boldsymbol{x}_2 d\boldsymbol{x}_1 \\ \leq \; & \lambda^2 \int_{A_{\frac{1}{r_\rho}}} \int_{A_{\frac{1}{r_\rho}} \cap D(\boldsymbol{x}_1,\delta)} e^{-\lambda\left(\int_{A_{\frac{1}{r_\rho}}} g(\|\boldsymbol{y}-\boldsymbol{x}_2\|)d\boldsymbol{y}+\left(\beta\sqrt{3}r-\pi\delta\right)\|\boldsymbol{x}_2-\boldsymbol{x}_1\|\right)} d\boldsymbol{x}_2 d\boldsymbol{x}_1 \\ = \; & \lambda^2 \int_{A_{\frac{1}{r_\rho}}} \int_{A_{\frac{1}{r_\rho}} \cap D(\boldsymbol{x}_2,\delta)} e^{-\lambda\left(\beta\sqrt{3}r-\pi\delta\right)\|\boldsymbol{x}_2-\boldsymbol{x}_1\|} d\boldsymbol{x}_1 e^{-\lambda\int_{A_{\frac{1}{r_\rho}}} g(\|\boldsymbol{y}-\boldsymbol{x}_2\|)d\boldsymbol{y}} d\boldsymbol{x}_2 \\ \leq \; & \frac{1-e^{-\lambda\left(\beta\sqrt{3}r-\pi\delta\right)\delta}\left(1+\lambda\left(\beta\sqrt{3}r-\pi\delta\right)\delta\right)}{\lambda\left(\beta\sqrt{3}r-\pi\delta\right)^2} \lambda \int_{A_\rho} e^{-\lambda\int_{A_{\frac{1}{r_\rho}}} g(\|\boldsymbol{y}-\boldsymbol{x}_2\|)d\boldsymbol{y}} d\boldsymbol{x}_2 \end{aligned}$$

In Theorem 1, we have established that

$$\lim_{\rho\to\infty} \lambda \int_{A_{\frac{1}{r_\rho}}} e^{-\lambda\int_{A_{\frac{1}{r_\rho}}} g(\|\boldsymbol{y}-\boldsymbol{x}_2\|)d\boldsymbol{y}} d\boldsymbol{x}_2 = e^{-b}$$

Therefore it follows straightforwardly that for $\delta < \beta\sqrt{3}r/\pi$

$$\lim_{\rho\to\infty} \lambda^2 \int_{A_{\frac{1}{r_\rho}} \backslash B_r\left(A_{\frac{1}{r_\rho}}\right)} \int_{A_{\frac{1}{r_\rho}} \cap D(\boldsymbol{x}_1,\delta)} e^{-\lambda\left(\int_{A_{\frac{1}{r_\rho}}} g(\|\boldsymbol{y}-\boldsymbol{x}_2\|)d\boldsymbol{y}+\beta\left|A_{\frac{1}{r_\rho}}\cap D(\boldsymbol{x}_1,r)\backslash D(\boldsymbol{x}_2,r)\right|-\pi\|\boldsymbol{x}_2-\boldsymbol{x}_1\|^2\right)} d\boldsymbol{x}_2 d\boldsymbol{x}_1 = 0 \tag{70}$$

Using (60), (61), (69) and (70), we are able to conclude that by chosing $\delta$ to be a positive constant such that

$$\delta < \min\left\{\frac{1}{4\pi}\gamma C, \frac{r}{2}, \frac{1}{2\pi}c_5\beta, \beta\sqrt{3}r/\pi, z_0\right\}$$

$$\lim_{\rho\to\infty} \sum_{k=2}^{\infty} E\left(\xi_{k,1}\right) = 0 \tag{71}$$

*An analysis of the second term in* (57)

Now let us consider the second term in (57), i.e.

$$\begin{aligned} & E\left(\xi_{k,2}\right) \\ = & \frac{\lambda^k}{k!}\int_{A_{\frac{1}{r\rho}}}\int_{\left(A_{\frac{1}{r\rho}}\right)^{k-1}\backslash\left(D\left(\boldsymbol{x}_1,\delta\right)\right)^{k-1}} g_1\left(\boldsymbol{x}_1,\boldsymbol{x}_2,\ldots,\boldsymbol{x}_k\right) e^{-\lambda\int_{A_{\frac{1}{r\rho}}} g_2\left(\boldsymbol{y};\boldsymbol{x}_1,\boldsymbol{x}_2,\ldots,\boldsymbol{x}_k\right)d\boldsymbol{y}} d\left(\boldsymbol{x}_2\cdots\boldsymbol{x}_k\right)d\boldsymbol{x}_1 \end{aligned}$$

For $\left(\boldsymbol{x}_2\cdots\boldsymbol{x}_k\right)\in\left(A_{\frac{1}{r\rho}}\right)^{k-1}\backslash\left(D\left(\boldsymbol{x}_1,\delta\right)\right)^{k-1}$, there is one node in $\{\boldsymbol{x}_2\cdots\boldsymbol{x}_k\}$ outside a Euclidean distance $\delta$ of $\boldsymbol{x}_1$ and belongs to $A_{\frac{1}{r\rho}}\backslash D\left(\boldsymbol{x}_1,\delta\right)$. Without losing generality, assume that node is $\boldsymbol{x}_j\in A_{\frac{1}{r\rho}}\backslash D\left(\boldsymbol{x}_1,\delta\right)$, where $j\in\Gamma_k/\{1\}$.

Let $\angle A_{\frac{1}{r\rho}}\subset A_{\frac{1}{r\rho}}$ be a square area of size $r\times r$ located at a corner of $A_{\frac{1}{r\rho}}$ as defined in the beginning of this Appendix and let $\overline{\angle A_{\frac{1}{r\rho}}}\subset A_{\frac{1}{r\rho}}$ be an area in $A_{\frac{1}{r\rho}}$ excluding the four corner squares $\angle A_{\frac{1}{r\rho}}$. It is straightforward from the proofs of Lemmas 8 and 7 that for $\boldsymbol{x}_1\in\overline{\angle A_{\frac{1}{r\rho}}}$ and $\boldsymbol{x}_j\in A_{\frac{1}{r\rho}}\backslash D\left(\boldsymbol{x}_1,\delta\right)$, i.e. $\|\boldsymbol{x}_j-\boldsymbol{x}_1\|\geq\delta$, there exists a positive constant $c_6>0$, depending on $\delta$, such that

$$\left|A_{\frac{1}{r\rho}}\cap D\left(\boldsymbol{x}_1,r\right)\backslash D\left(\boldsymbol{x}_2,r\right)\right|\geq c_6$$

Using the above inequality and (52), it follows that

$$\begin{aligned} & \int_{A_{\frac{1}{r\rho}}} g_2\left(\boldsymbol{y};\boldsymbol{x}_1,\boldsymbol{x}_2,\ldots,\boldsymbol{x}_k\right)d\boldsymbol{y} \\ \geq & \int_{A_{\frac{1}{r\rho}}} g_2\left(\boldsymbol{y};\boldsymbol{x}_1,\boldsymbol{x}_j\right)d\boldsymbol{y} \\ = & \int_{A_{\frac{1}{r\rho}}} g\left(\|\boldsymbol{y}-\boldsymbol{x}_j\|\right)+g\left(\|\boldsymbol{y}-\boldsymbol{x}_1\|\right)\left(1-g\left(\|\boldsymbol{y}-\boldsymbol{x}_j\|\right)\right)d\boldsymbol{y} \\ \geq & \int_{A_{\frac{1}{r\rho}}} g\left(\|\boldsymbol{y}-\boldsymbol{x}_j\|\right)d\boldsymbol{y}+\beta\left|A_{\frac{1}{r\rho}}\cap D\left(\boldsymbol{x}_1,r\right)\backslash D\left(\boldsymbol{x}_j,r\right)\right| \\ \geq & \int_{A_{\frac{1}{r\rho}}} g\left(\|\boldsymbol{y}-\boldsymbol{x}_j\|\right)d\boldsymbol{y}+\beta c_6 \end{aligned}$$

Therefore

$$\begin{aligned} & \frac{\lambda^k}{k!}\int_{\overline{\angle A_{\frac{1}{r\rho}}}}\int_{\left(A_{\frac{1}{r\rho}}\right)^{k-1}\backslash\left(D\left(\boldsymbol{x}_1,\delta\right)\right)^{k-1}} g_1\left(\boldsymbol{x}_1,\boldsymbol{x}_2,\ldots,\boldsymbol{x}_k\right)e^{-\lambda\int_{A_{\frac{1}{r\rho}}} g_2\left(\boldsymbol{y};\boldsymbol{x}_1,\boldsymbol{x}_2,\ldots,\boldsymbol{x}_k\right)d\boldsymbol{y}} d\left(\boldsymbol{x}_2\cdots\boldsymbol{x}_k\right)d\boldsymbol{x}_1 \\ \leq & \frac{\lambda^k}{k!}\int_{\overline{\angle A_{\frac{1}{r\rho}}}}\int_{\left(A_{\frac{1}{r\rho}}\right)^{k-1}\backslash\left(D\left(\boldsymbol{x}_1,\delta\right)\right)^{k-1}} g_1\left(\boldsymbol{x}_1,\boldsymbol{x}_2,\ldots,\boldsymbol{x}_k\right)e^{-\lambda\int_{A_{\frac{1}{r\rho}}} g\left(\|\boldsymbol{y}-\boldsymbol{x}_j\|\right)d\boldsymbol{y}-\lambda\beta c_6} d\left(\boldsymbol{x}_2\cdots\boldsymbol{x}_k\right)d\boldsymbol{x}_1 \\ \leq & \frac{\lambda^k}{k!}\int_{\left(A_{\frac{1}{r\rho}}\right)^k} g_1\left(\boldsymbol{x}_1,\boldsymbol{x}_2,\ldots,\boldsymbol{x}_k\right)e^{-\lambda\int_{A_{\frac{1}{r\rho}}} g\left(\|\boldsymbol{y}-\boldsymbol{x}_j\|\right)d\boldsymbol{y}-\lambda\beta c_6} d\left(\boldsymbol{x}_1\boldsymbol{x}_2\cdots\boldsymbol{x}_k\right) \\ = & \frac{\lambda^k}{k!}\int_{\left(A_{\frac{1}{r\rho}}\right)^k} g_1\left(\boldsymbol{x}_1,\boldsymbol{x}_2,\ldots,\boldsymbol{x}_k\right)e^{-\lambda\int_{A_{\frac{1}{r\rho}}} g\left(\|\boldsymbol{y}-\boldsymbol{x}_1\|\right)d\boldsymbol{y}-\lambda\beta c_6} d\left(\boldsymbol{x}_1\boldsymbol{x}_2\cdots\boldsymbol{x}_k\right) \end{aligned} \tag{72}$$

where a re-numbering of the nodes occurred in the last step of the above equation. First using Lemma 6, and then using (53) and the inequality that $\int_{A_{\frac{1}{r\rho}}} g\left(\|\boldsymbol{x}_j-\boldsymbol{x}_i\|\right)d\boldsymbol{x}_i\leq C$, it can be shown that

$$\begin{aligned} & \frac{\lambda^k}{k!}\int_{\left(A_{\frac{1}{r\rho}}\right)^k} g_1\left(\boldsymbol{x}_1,\boldsymbol{x}_2,\ldots,\boldsymbol{x}_k\right)e^{-\lambda\int_{A_{\frac{1}{r\rho}}} g\left(\|\boldsymbol{y}-\boldsymbol{x}_1\|\right)d\boldsymbol{y}-\lambda\beta c_6} d\left(\boldsymbol{x}_1\boldsymbol{x}_2\cdots\boldsymbol{x}_k\right) \\ \leq & \frac{\lambda^k}{k!}\int_{\left(A_{\frac{1}{r\rho}}\right)^k}\sum_{i_2\in\Gamma_k\backslash\{1\},\cdots,i_k\in\Gamma_k\backslash\{1,i_2,\ldots,i_{k-1}\}} g_2\left(\boldsymbol{x}_{i_2};\boldsymbol{x}_1\right)\cdots g_2\left(\boldsymbol{x}_{i_k};\boldsymbol{x}_1,\boldsymbol{x}_{i_2},\ldots,\boldsymbol{x}_{i_{k-1}}\right) \\ \times & e^{-\lambda\int_{A_{\frac{1}{r\rho}}} g\left(\|\boldsymbol{y}-\boldsymbol{x}_1\|\right)d\boldsymbol{y}-\lambda\beta c_6} d\left(\boldsymbol{x}_{i_k}\cdots\boldsymbol{x}_{i_2}\boldsymbol{x}_1\right) \end{aligned}$$

$$\begin{aligned}
&\le \frac{\lambda^k C^{k-1}}{k!}(k-1)!\,(k-1)!\int_{A_{\frac{1}{r_\rho}}} e^{-\lambda\int_{A_{\frac{1}{r_\rho}}} g(\|\boldsymbol{y}-\boldsymbol{x}_1\|)d\boldsymbol{y}-\lambda\beta c_6} d\boldsymbol{x}_1 \\
&= \frac{(k-1)!}{k} e^{-\frac{b\beta c_6}{C}} \times \frac{(\log\rho + b)^{k-1}}{\rho^{\frac{\beta c_6}{C}}} \times \lambda \int_{A_{\frac{1}{r_\rho}}} e^{-\lambda\int_{A_\rho} g(\|\boldsymbol{y}-\boldsymbol{x}_1\|)d\boldsymbol{y}} d\boldsymbol{x}_1 \qquad (73)
\end{aligned}$$

Using Theorem 1, (72) and (73), it follows that

$$\lim_{\rho\to\infty}\frac{\lambda^k}{k!}\int_{\angle A_{\frac{1}{r_\rho}}}\int_{\left(A_{\frac{1}{r_\rho}}\right)^{k-1}\setminus(D(\boldsymbol{x}_1,\delta))^{k-1}} g_1(\boldsymbol{x}_1,\boldsymbol{x}_2,\ldots,\boldsymbol{x}_k)\, e^{-\lambda\int_{A_{\frac{1}{r_\rho}}} g_2(\boldsymbol{y};\boldsymbol{x}_1,\boldsymbol{x}_2,\ldots,\boldsymbol{x}_k)d\boldsymbol{y}} d(\boldsymbol{x}_2\cdots\boldsymbol{x}_k)\,d\boldsymbol{x}_1 = 0 \qquad (74)$$

Using similar steps as those leading to (73), it can be shown that

$$\begin{aligned}
&\frac{\lambda^k}{k!}\int_{\angle A_{\frac{1}{r_\rho}}}\int_{\left(A_{\frac{1}{r_\rho}}\right)^{k-1}\setminus(D(\boldsymbol{x}_1,\delta))^{k-1}} g_1(\boldsymbol{x}_1,\boldsymbol{x}_2,\ldots,\boldsymbol{x}_k)\, e^{-\lambda\int_{A_{\frac{1}{r_\rho}}} g_2(\boldsymbol{y};\boldsymbol{x}_1,\boldsymbol{x}_2,\ldots,\boldsymbol{x}_k)d\boldsymbol{y}} d(\boldsymbol{x}_2\cdots\boldsymbol{x}_k)\,d\boldsymbol{x}_1 \\
\le\ &\frac{\lambda^k}{k!}\int_{\angle A_{\frac{1}{r_\rho}}}\int_{\left(A_{\frac{1}{r_\rho}}\right)^{k-1}} g_1(\boldsymbol{x}_1,\boldsymbol{x}_2,\ldots,\boldsymbol{x}_k)\, e^{-\lambda\int_{A_{\frac{1}{r_\rho}}} g_2(\|\boldsymbol{y}-\boldsymbol{x}_1\|)d\boldsymbol{y}} d(\boldsymbol{x}_2\cdots\boldsymbol{x}_k)\,d\boldsymbol{x}_1 \\
\le\ &\frac{\lambda^k C^{k-1}}{k}(k-1)!\int_{\angle A_{\frac{1}{r_\rho}}} e^{-\lambda\int_{A_{\frac{1}{r_\rho}}} g(\|\boldsymbol{y}-\boldsymbol{x}_1\|)d\boldsymbol{y}} d\boldsymbol{x}_1
\end{aligned}$$

Using similar steps that resulted in (68), it can be shown that

$$\begin{aligned}
&\lim_{\rho\to\infty}\frac{\lambda^k C^{k-1}}{k}(k-1)!\int_{\angle A_{\frac{1}{r_\rho}}} e^{-\lambda\int_{A_{\frac{1}{r_\rho}}} g(\|\boldsymbol{y}-\boldsymbol{x}_1\|)d\boldsymbol{y}-\lambda\beta c_6} d\boldsymbol{x}_1 \\
\le\ &\lim_{\rho\to\infty}\frac{\lambda^k C^{k-1}}{k}(k-1)!\delta^2 e^{-\frac{1}{4}\lambda\gamma C} \\
=\ &0 \qquad (75)
\end{aligned}$$

The combination of (74) and (75) allows us to conclude that

$$\lim_{\rho\to\infty} E(\xi_{k,2}) = 0$$

It follows that for any fixed but arbitrarily large integer $M$

$$\lim_{\rho\to\infty}\sum_{k=2}^{M} E(\xi_{k,2}) = 0 \qquad (76)$$

Finally from (71) and (76), we conclude that

$$\lim_{\rho\to\infty}\left(\sum_{k=2}^{M} E(\xi_k) = 0\right) = 0$$

Noting that $\xi_k$ is a non-negative integer, therefore

$$\lim_{\rho\to\infty}\Pr\left(\sum_{k=2}^{M}\xi_k = 0\right) = 1$$

## ACKNOWLEDGMENT

The authors would like to thank Prof P. R. Kumar of University of Illinois, Urbana-Champaign for his comments on an earlier version of this paper.

## REFERENCES


[1] M. Haenggi, J. G. Andrews, F. Baccelli, O. Dousse, and M. Franceschetti, "Stochastic geometry and random graphs for the analysis and design of wireless networks," *IEEE Journal on Selected Areas in Communications*, vol. 27, no. 7, pp. 1029–1046, 2009.

[2] R. Meester and R. Roy, *Continuum Percolation*, ser. Cambridge Tracts in Mathematics. Cambridge University Press, 1996.

[3] P. Gupta and P. R. Kumar, "Critical power for asymptotic connectivity in wireless networks," in *Stochastic Analysis, Control, Optimization and Applications*. Boston, MA: Birkhauser, 1998, pp. 547–566.

[4] X. Ta, G. Mao, and B. D. Anderson, "On the giant component of wireless multi-hop networks in the presence of shadowing," *IEEE Transactions on Vehicular Technology*, vol. 58, no. 9, pp. 5152–5163, 2009.

[5] Z. Kong and E. M. Yeh, "Connectivity and latency in large-scale wireless networks with unreliable links," in *IEEE INFOCOM*, 2008, pp. 11–15.

[6] D. Goeckel, L. Benyuan, D. Towsley, W. Liaoruo, and C. Westphal, "Asymptotic connectivity properties of cooperative wireless ad hoc networks," *IEEE Journal on Selected Areas in Communications*, vol. 27, no. 7, pp. 1226–1237, 2009.

[7] H. M. Ammari and S. K. Das, "Integrated coverage and connectivity in wireless sensor networks: A two-dimensional percolation problem," *IEEE Transactions on Computers*, vol. 57, no. 10, pp. 1423–1434, 2008.

[8] P. Li, C. Zhang, and Y. Fang, "Asymptotic connectivity in wireless ad hoc networks using directional antennas," *IEEE/ACM Transactions on Networking*, vol. 17, no. 4, pp. 1106–1117, 2009.

[9] M. D. Penrose, "On k-connectivity for a geometric random graph," *Random Structures and Algorithms*, vol. 15, no. 2, pp. 145–164, 1999.

[10] ——, *Random Geometric Graphs*, ser. Oxford Studies in Probability. Oxford University Press, USA, 2003.

[11] F. Xue and P. Kumar, "The number of neighbors needed for connectivity of wireless networks," *Wireless Networks*, vol. 10, no. 2, pp. 169–181, 2004.

[12] T. K. Philips, S. S. Panwar, and A. N. Tantawi, "Connectivity properties of a packet radio network model," *IEEE Transactions on Information Theory*, vol. 35, no. 5, pp. 1044–1047, 1989.

[13] V. Ravelomanana, "Extremal properties of three-dimensional sensor networks with applications," *IEEE Transactions on Mobile Computing*, vol. 3, no. 3, pp. 246–257, 2004.

[14] P. Balister, B. Bollobas, A. Sarkar, and M. Walters, "Connectivity of random k-nearest-neighbour graphs," *Advances in Applied Probability*, vol. 37, no. 1, pp. 1–24, 2005.

[15] P.-J. Wan and C.-W. Yi, "Asymptotic critical transmission radius and critical neighbor number for k-connectivity in wireless ad hoc networks," 2004.

[16] P. Balister, B. Bollobas, A. Sarkar, and M. Walters, "A critical constant for the k nearest neighbour model," *Advances in Applied Probability*, vol. 41, no. 1, pp. 1–12, 2009.

[17] M. Penrose, "The longest edge of the random minimal spanning tree," *The Annals of Applied Probability*, vol. 7, no. 2, pp. 340–361, 1997.

[18] ——, "A strong law for the longest edge of the minimal spanning tree," *The Annals of Applied Probability*, vol. 27, no. 1, pp. 246–260, 1999.

[19] R. Hekmat and P. V. Mieghem, "Connectivity in wireless ad-hoc networks with a log-normal radio model," *Mobile Networks and Applications*, vol. 11, no. 3, pp. 351–360, 2006.

[20] J. Orriss and S. K. Barton, "Probability distributions for the number of radio transceivers which can communicate with one another," *EEE Transactions on Communications*, vol. 51, no. 4, pp. 676–681, 2003.

[21] D. Miorandi and E. Altman, "Coverage and connectivity of ad hoc networks presence of channel randomness," in *IEEE INFOCOM*, vol. 1, 2005, pp. 491–502.

[22] D. Miorandi, "The impact of channel randomness on coverage and connectivity of ad hoc and sensor networks," *IEEE Transactions on Wireless Communications*, vol. 7, no. 3, pp. 1062–1072, 2008.

[23] C. Bettstetter, "Failure-resilient ad hoc and sensor networks in a shadow fading environment," in *IEEE/IFIP International Conference on Dependable Systems and Networks*, 2004.

[24] C. Bettstetter and C. Hartmann, "Connectivity of wireless multihop networks in a shadow fading environment," *Wireless Networks*, vol. 11, no. 5, pp. 571–579, 2005.

[25] T. S. Rappaport, *Wireless Communications: Principles and Practice*, ser. Prentice Hall Communications Engineering and Emerging Technologies Series. Prentice Hall, 2002.

[26] O. Dousse, F. Baccelli, and P. Thiran, "Impact of interferences on connectivity in ad hoc networks," *IEEE/ACM Transactions on Networking*, vol. 13, no. 2, pp. 425–436, 2005.

[27] M. Franceschetti and R. Meester, *Random Networks for Communication*. Cambridge University Press, 2007.

[28] M. Franceschetti, O. Dousse, D. N. C. Tse, and P. Thiran, "Closing the gap in the capacity of wireless networks via percolation theory," *IEEE Transactions on Information Theory*, vol. 53, no. 3, pp. 1009–1018, 2007.

[29] G. Mao, B. Fidan, and B. D. O. Anderson, "Wireless sensor network localization techniques," *Computer Networks*, vol. 51, no. 10, pp. 2529–2553, 2007.

[30] J. L. Gross and J. Yellen, *Handbook of Graph Theory*, 2004.

[31] O. Dousse, F. Baccelli, and P. Thiran, "Impact of interferences on connectivity in ad hoc networks," in *IEEE INFOCOM*, vol. 3, 2003, pp. 1724–1733.

[32] G. Mao and B. D. Anderson, "On the asymptotic connectivity of random networks under the random connection model," in *IEEE INFOCOM*, 2011, pp. 1–9.

[33] M. D. Penrose, "On a continuum percolation model," *Advances in Applied Probability*, no. 23, pp. 536–556, 1991.


PLACE PHOTO HERE

**Guoqiang Mao** (S'98–M'02–SM'08) received PhD in telecommunications engineering in 2002 from Edith Cowan University. He joined the School of Electrical and Information Engineering, the University of Sydney in December 2002 where he is a Senior Lecturer now. His research interests include wireless localization techniques, wireless multihop networks, graph theory and its application in networking, and network performance analysis. He is a Senior Member of IEEE and an Associate Editor of IEEE Transactions on Vehicular Technology.

PLACE PHOTO HERE

**Brian D.O. Anderson** (S'62–M'66–SM'74–F'75– LF'07) was born in Sydney, Australia, and educated at Sydney University in mathematics and electrical engineering, with PhD in electrical engineering from Stanford University in 1966. He is a Distinguished Professor at the Australian National University and Distinguished Researcher in National ICT Australia. His awards include the IEEE Control Systems Award of 1997, the 2001 IEEE James H Mulligan, Jr Education Medal, and the Bode Prize of the IEEE Control System Society in 1992, as well as several IEEE best paper prizes. He is a Fellow of the Australian Academy of Science, the Australian Academy of Technological Sciences and Engineering, the Royal Society, and a foreign associate of the National Academy of Engineering. His current research interests are in distributed control, sensor networks and econometric modelling.